

2016•2017
FACULTEIT GENEESKUNDE EN LEVENSWETENSCHAPPEN
master in de biomedische wetenschappen

Masterproef

Dental paediatric imaging: an investigation into low dose radiation-induced risks

Promotor :
Prof. dr. Ivo LAMBRICHTS

Promotor :
dr. MARJAN MOREELS

Liese Gilles

Scriptie ingediend tot het behalen van de graad van master in de biomedische wetenschappen

De transnationale Universiteit Limburg is een uniek samenwerkingsverband van twee universiteiten in twee landen: de Universiteit Hasselt en Maastricht University.



Universiteit Hasselt | Campus Hasselt | Martelarenlaan 42 | BE-3500 Hasselt
Universiteit Hasselt | Campus Diepenbeek | Agoralaan Gebouw D | BE-3590 Diepenbeek



2016•2017
FACULTEIT GENEESKUNDE EN
LEVENSWETENSCHAPPEN
master in de biomedische wetenschappen

Masterproef

Dental paediatric imaging: an investigation into low
dose radiation-induced risks

Promotor :
Prof. dr. Ivo LAMBRICHTS

Promotor :
dr. MARJAN MOREELS

Liese Gilles

*Scriptie ingediend tot het behalen van de graad van master in de biomedische
wetenschappen*

Table of Contents

Table of Contents	I
List of figures	V
List of tables	VII
List of supplements	IX
List of abbreviations	XI
Acknowledgements	XIII
Samenvatting.....	XV
Summary	XVII
1 Introduction.....	1
1.1 Radiation sources	1
1.1.1 Evolution of medical radiation exposure	1
1.2 History and advances of X-rays in dentistry.....	2
1.3 Dental cone beam computed tomography.....	3
1.3.1 Radiation doses	3
1.3.2 Radiation doses associated with dental CBCT	3
1.4 Biological effects of ionizing radiation	4
1.4.1 Oxidative stress after ionizing radiation	4
1.4.2 Types of DNA damage after ionizing radiation	5
1.4.3 The role of γ H2AX and 53BP1 in DNA damage response.....	5
1.5 Importance of radiation protection	6
1.5.1 Radiation protection in children	7
1.6 Low dose radiation hypothesis	7
1.7 Preliminary data	8
1.8 Experimental approach	9
2 Materials and methods	11
2.1 Participants.....	11
2.2 Sample collection of saliva and exfoliated oral mucosa cells	11
2.2.1 Harvesting and fixation of exfoliated oral mucosa cells	12
2.3 Cell cultures.....	13
2.3.1 Isolation and culture of paediatric dental stem cells.....	13
2.3.2 Culture of PC3, A431, TICAЕ and Jurkat cells.	13

2.4	<i>In vitro</i> X-irradiation of dental pulp stem cells, stem cells of the apical papilla and dental follicle stem cells.....	13
2.5	Analysis of DNA DSBs with γ H2AX and 53BP1 immunocytochemical staining.....	14
2.5.1	Fixation of dental stem cells and collection of supernatant.....	14
2.5.2	Immunocytochemistry for γ H2AX and 53BP1.....	14
2.5.3	Fluorescence microscopy: γ H2AX and 53BP1 co-localized foci analysis	15
2.6	Ferric Reducing Antioxidant Power (FRAP) assay	15
2.7	8-Hydroxy-2'-deoxyguanosine (8-OHdG) determination in saliva and supernatant	15
2.7.1	Purification of saliva and supernatant	15
2.7.2	Elution of 8-OHdG	16
2.7.3	Enzyme linked immunosorbent assay (ELISA): 8-OHdG.....	16
2.8	Analysis of buccal swab composition.....	17
2.8.1	Analysis of buccal swab composition using flow cytometry.....	17
2.8.2	Giemsa staining of buccal swab	17
2.9	Statistical analysis.....	18
3	Results	19
3.1	Biological response of paediatric dental stem cells after low dose <i>in vitro</i> radiation exposure	19
3.1.1	DNA DSB induction and repair after X-ray exposure in dental stem cells.	19
3.1.2	8-OHdG in supernatant of dental stem cells after <i>in vitro</i> X-ray exposure using an ELISA-assay	21
3.1.3	Total antioxidant capacity of supernatant of SCAP after <i>in vitro</i> X-ray exposure using a FRAP-assay.....	21
3.2	DNA double strand breaks in exfoliated oral mucosa cells after clinical dental CBCT exposure	22
3.2.1	Characterization of buccal swab composition using flow cytometry	22
3.2.2	DNA DSB induction in exfoliated oral mucosa cells after clinical dental CBCT exposure	24
3.3	Measurement of oxidative stress in saliva after clinical dental CBCT exposure	25
3.3.1	Measurement of 8-OHdG concentration in saliva with an ELISA-assay	25

3.3.2	Measurement of total antioxidant capacity of saliva after clinical dental CBCT exposure with a FRAP-assay.....	26
4	Discussion.....	29
4.1	Biological response of dental stem cells after low dose irradiation (<i>in vitro</i>)	29
4.1.1	DNA DSB induction and repair in dental stem cells after <i>in vitro</i> X-ray exposure	29
4.1.2	Total antioxidant capacity of supernatant of SCAP after <i>in vitro</i> X-ray exposure	30
4.1.3	Concentration of 8-OHdG in supernatant of SCAP after X-ray exposure (<i>in vitro</i>).....	31
4.2	DNA damage in exfoliated oral mucosa cells of children and adults after dental CBCT exposure	31
4.2.1	Composition of buccal swabs.....	31
4.2.2	DNA DSBs in exfoliated oral mucosa cells of children and adults after dental CBCT exposure	31
4.3	Oxidative stress in saliva after dental CBCT exposure	33
4.3.1	Salivary 8-OHdG concentration after dental CBCT exposure in children and adults....	34
4.3.2	Total antioxidant capacity of saliva after clinical dental CBCT exposure.....	35
5	Conclusion	37
6	Literature references.....	39
7	Supplemental information	43

List of figures

Figure 1: Evolution of the annual average radiation dose per person (mSv) in the USA population.....	1
Figure 2: Graphical representation of the different models explaining the dose-response relationship within the low dose range (<100 mGy).....	8
Figure 3: γ H2AX and 53BP1 repair kinetics after low dose X-irradiation (<i>in vitro</i>).....	8
Figure 4: DNA DSB induction and repair after low dose X-ray exposure <i>in vitro</i> in dental stem cells.	20
Figure 5: Total antioxidant capacity of supernatant of SCAP after low dose <i>in vitro</i> X-ray exposure..	21
Figure 6: Flow cytometric characterization of buccal swab composition.	23
Figure 7: Number of DNA DSBs before and after dental CBCT exposure in exfoliated oral mucosa cells of children and adults.....	24
Figure 8: Salivary 8-OHdG concentration before and after clinical dental CBCT exposure in children and adults.....	25
Figure 9: Total antioxidant capacity before and after clinical dental CBCT exposure in children and adults.....	27

List of tables

Table 1: Trend in radiation exposure from diagnostic radiology (4) 2

Table 2: Specifications of the dental CBCT units used in the different hospitals and the number of patients..... 12

Table 3: Age and gender of dental stem cell donors. 13

Table 4: Overview of the used antibodies. 18

List of supplements

Supplementary figure 1: Annual average exposure to ionizing radiation and the associated contribution of different radiation sources. 43

Supplementary figure 2: 2D and 3D images of the oral and maxillofacial region. 43

Supplementary table 1: Typical effective dose associated with diagnostic imaging examinations (2).
..... 44

Supplementary figure 3: Direct and indirect effects of ionizing radiation on DNA. 44

Supplementary figure 4: Automated foci count using FIJI software. 45

Supplementary figure 5: Dose response relationship of DPSC, DFSC and SCAPs 30 min, 1 h, 4 hrs and 24 hrs p.i. 46

Supplementary figure 6: Comparison of basal DNA DSB occurrence and radiation sensitivity between children and adults. 46

Supplementary figure 7: Comparison of basal salivary 8-OHdG and radiation sensitivity between children and adults. 47

Supplementary figure 8: Meta-analysis of total antioxidant capacity data in saliva before and after dental CBCT exposure. 48

List of abbreviations

53BP1	53 binding protein 1	NHEJ	non-homologous end rejoining
7-AAD	7-AminoActinomycin D		
ALARA	as low as reasonably achievable	OMF	oral and maxillofacial
		ORAC	oxygen radical antioxidant capacity
ATM	ataxia-telangiectasia mutated		
BuBu	buccal cell buffer	p.i.	post irradiation
CBCT	cone beam computerized tomography	PBS	phosphate buffered saline
		PBS	phosphate buffered saline
CD45	cluster of differentiation 45	PFA	paraformaldehyde
CK-4	cytokeratin 4	ROS	reactive oxygen species
DDR	DNA damage response	RPMI	Roswell Park Memorial Institute medium
DFSC	dental follicle stem cells		
DMEM	Dulbecco's modified Eagle medium	RT	room temperature
		SCAP	stem cells of apical papilla
DNA	deoxyribonucleic acid	SSB	single strand break
DPSC	dental pulp stem cells	Sv	Sievert
DSB	double strand break	TAC	total antioxidant capacity
DSB	double strand break	TBST	tris-buffered saline with tween 20
ELISA	enzyme linked immunosorbent assay	TEAC	trolox equivalent antioxidant capacity
FBS	fetal bovine serum		
FDA	federal drug agency	TICAE	telomerase immortalized human coronary artery endothelial cells
FOV	field of view		
FRAP	ferric reducing anti-oxidant potential	TRAP	total radical-trapping antioxidant parameter
Gy	gray		
HR	homologous recombination	γ H2AX	phosphorylated histone H2A variant X
IR	ionizing radiation		
LNT	linear-no-threshold		
MRN	MRE11–RAD50–NBS1 (protein complex)		

Acknowledgements

I would like to take this opportunity to express my gratitude to several people. First of all, I would like to thank all the people of the Radiobiology and Microbiology unit at SCK•CEN for their warm welcome. Prof. dr. Sarah Baatout, thank you for giving me the opportunity to work in the lab of the SCK•CEN Radiobiology Unit. It was a great experience in a great environment!

This study would not have been possible without the provision of patients' material by prof. Jacobs (KU Leuven, Belgium), dr. Benjamin Salmon (Université Paris Descartes, France) and prof. Mihaela Hedesiu and prof. Piroska Virag (Cluj Napoca, Romania).

In addition, I would like to thank Prof. dr. I. Lambrichts, dr. Marjan Moreels, drs. Niels Belmans and prof. dr. Bronckaers. I am especially grateful to my daily supervisor Niels Belmans for teaching me the experimental techniques and for his help during data analysis. Thank you for guiding me through my internship and thesis. Marjan thank you for your advice and suggestions during our weekly meetings.

And of course, a big thank you goes out to all the other students at SCK•CEN for all the help, encouragements and advice and for keeping me up to date with the latest gossip! I really enjoyed the funny conversations and all the coffee breaks, lunch breaks and after work drinks ;). Last but not least, I would like to thank my family and friends for their support and friendship.

Samenvatting

Het gebruik van cone beam CT (CBCT) als diagnostische tool binnen de tandheelkunde heeft de laatste jaren enorm aan populariteit gewonnen, vooral in de pediatrische orthodontie. Ondanks het feit dat CBCT wordt beschouwd als een lage dosis beeldvorming modaliteit, is het niet geweten of blootstelling aan lage dosis straling negatieve gezondheidsgevolgen veroorzaakt. Vooral bij kinderen is deze vraagstelling belangrijk omdat zij doorgaans gevoeliger zijn voor straling dan volwassenen. Onze hypothese stelt dat blootstelling aan lage dosis ioniserende straling, zoals gebruikt wordt in dentale CBCT, DNA schade en oxidatieve stress induceert in dentale stamcellen (*in vitro*) en in orale mucosa cellen en speeksel (*ex vivo*) op een leeftijdsafhankelijke manier.

Drie verschillende dentale stamcel types (dentale pulpa stamcellen, stamcellen van de apicale papilla en dentale follikel stamcellen) werden geïsoleerd bij kinderen en blootgesteld aan lage dosis ioniserende straling (0, 5, 10, 20, 50, 100 mGy). Oxidatieve stress en de inductie en herstel van dubbelstrengs DNA breuken werden geanalyseerd op verschillende tijdstippen na bestraling. Daarnaast werden ook orale mucosa cellen en speekselstalen verzameld bij kinderen en volwassenen. Hierin werd de frequentie van dubbelstrengs DNA breuken en oxidatieve stress vergeleken tussen stalen genomen voor en na CBCT blootstelling.

Onze resultaten toonden aan dat de frequentie van dubbelstrengs DNA breuken verhoogt met toenemende dosis (0 – 100 mGy). 0,5 - 1 uur na bestraling werd een piek respons geobserveerd waarna het aantal DNA dubbelstrengs breuken geleidelijk afneemt tot basale levels 24 uur na bestraling. Onze *ex vivo* resultaten toonden aan dat zowel bij kinderen als volwassenen het aantal dubbelstrengs DNA breuken in orale mucosa cellen niet significant toeneemt na blootstelling aan CBCT. Tot slot, nam de concentratie 8-OHdG significant toe in het speeksel van kinderen na blootstelling aan CBCT.

We kunnen concluderen dat onze *in vitro* resultaten de lineaire dosis-respons relatie ondersteund in dentale stamcellen. Daarnaast blijkt dentale CBCT niet significant meer DNA dubbelstrengs breuken te induceren in kinderen en in volwassenen. Maar de inductie van oxidatieve DNA schade (8-OHdG) is wel hoger in speekselstalen van kinderen dan van volwassenen. Tot slot dragen de resultaten van deze studie bij tot een beter begrip van de potentiële biologische effecten van dentale CBCT, zowel bij kinderen als volwassenen.

Summary

During the last decade dental cone beam CT (CBCT) has become a popular diagnostic tool in paediatric dentistry. Although dental CBCT is considered a low dose imaging modality, it remains uncertain whether low dose radiation exposure causes adverse health effects. This is especially important regarding children as they are more sensitive to ionizing radiation than adults. Therefore, we hypothesize that low dose radiation exposure, as used in dental CBCT, induces DNA damage and oxidative stress, in dental stem cells (*in vitro*) and in buccal cells and saliva (*ex vivo*) in an age-dependent manner.

Dental pulp stem cells, stem cells of the apical papilla and dental follicle stem cells were isolated from children and irradiated *in vitro* with low dose (0, 5, 10, 20, 50, 100 mGy) ionizing radiation. After X-ray exposure, oxidative stress and the induction and repair kinetics of DNA double strand breaks (DSBs) were analysed at multiple time points. Furthermore, exfoliated oral mucosa cells and saliva were collected, from children and adults, to compare the frequency of DNA DSBs and the level of oxidative stress before and after dental CBCT exposure.

We observed that the frequency of DNA DSBs increased with the dose (0 - 100 mGy) with a peak response 0.5 - 1 hour post irradiation (p.i.), after which the number of DNA DSBs continuously decreased returning to basal levels 24 hrs p.i.. Our *ex vivo* data revealed that in both children and adults, dental CBCT exposure did not significantly increase the number of DNA DSBs 30 minutes and 24 hrs after exposure. Finally, only in children, a significant increase in salivary 8-OHdG concentration was observed after dental CBCT exposure.

In summary, our results support the linear no-threshold dose-response relationship as observed in dental stem cells exposed to low dose X-irradiation (*in vitro*). Furthermore, it appears that dental CBCT does not induce significantly more DNA DSBs in children and adults, but induces significantly more oxidative DNA damage (8-OHdG) in children. The results of this study contribute to a better understanding of the potential biological effects of dental CBCT in children and adults.

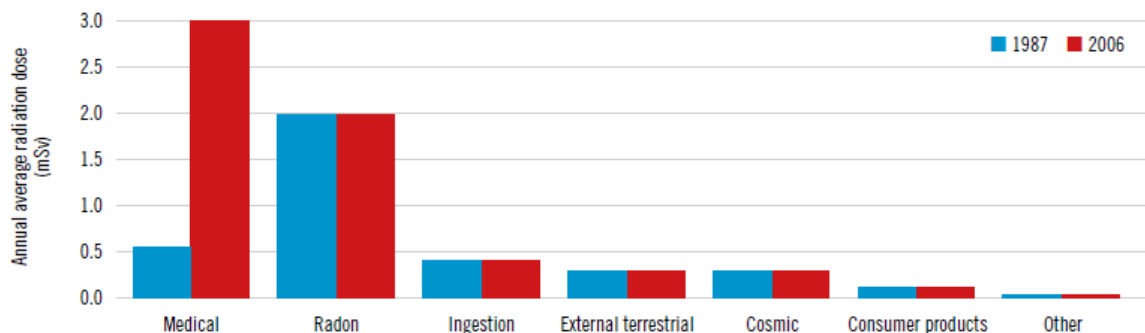
1 Introduction

1.1 Radiation sources

The average annual exposure to ionizing radiation (IR) in Belgium is 5.06 mSv/caput/year (1). This IR exposure originates from several sources. Every day we are exposed to natural background radiation, which is caused by cosmic radiation and the presence of radioactive elements in our environment, such as radon gas. Besides these natural sources, we are also exposed to radiation of man-made origin. The most important source of artificial radiation exposure is medical radiation exposure, which includes diagnostic imaging and nuclear medicine (1).

1.1.1 Evolution of medical radiation exposure

About 20 years ago, the contribution of medical radiation exposure to the annual collective dose was estimated to be around 25-30% in Belgium. Nowadays, medical radiation exposure is the largest controllable radiation source, which has a contribution of 45.8% in Belgium and 19.8% worldwide to the average annual exposure (see Supplementary figure 1). As an example, in the American population the medical radiation exposure has risen from 0.5 mSv/caput/year to 3.0 mSv/caput/year (1987 - 2006), whilst the contribution of other sources (radon, cosmic, industrial,...) has remained stable over the same time period (see Figure 1) (2).



Source: Adapted, with permission, from NCRP (2009)

Figure 1: Evolution of the annual average radiation dose per person (mSv) in the USA population.

Over a period of 20 years the annual average radiation dose per person in the USA population has increased. Especially the proportion of medical radiation exposure (not including radiotherapy) has strongly increased, whilst radiation originating from other sources like radon, ingestion of radioactive nutrition, external terrestrial radiation, cosmic radiation etc. has remained stable (2).

Although newly developed X-ray technologies, like dental cone beam CT (CBCT), have significantly improved the quality of medical imaging, the downside is that they are causing an extremely rapid increase in the annual collective population dose. This strong increase can be explained by two main factors: 1) an increase in the number of diagnostic procedures utilising X-rays, 2) an increase of the doses associated with the new X-ray technologies that are used (3). This increasing trend in radiation exposure from diagnostic radiology was reported by the United Nations in their UNSCEAR report

(2008). They observed that since their previous survey (covering the period 1991 – 1996), the total number of diagnostic medical examinations, is estimated to have risen from 2.4 billion to 3.6 billion which accounts for an increase of approximately 50% (Table 1) (4).

Table 1: Trend in radiation exposure from diagnostic radiology (4)

Year of Committee report in which survey data were analysed	Number of examination (millions)	Collective effective dose (man Sv)	Annual per caput dose (mSv)
1988	1 380	1 800 000	0.35
1993	1 600	1 600 000	0.3
2000	1 910	2 300 000	0.4
2008	3 100	4 000 000	0.6

However, it is not only the increasing number of examinations that contributes to the increasing population dose. The doses that are associated with these newer techniques are also higher compared to the classical 2D-radiography techniques (see paragraph 1.3.2.). These two factors combined have caused the average annual radiation exposure to increase over the last two decades which has concerned physicians and radiation physicists, as well as regulatory bodies and politicians (4).

1.2 History and advances of X-rays in dentistry

The use of ionizing radiation for medical imaging began in 1895 when Wilhelm Conrad Roentgen accidentally discovered the X-rays (5, 6). Roentgen’s discovery was a scientific breakthrough. Health care professionals immediately recognized the tremendous benefits of his discovery, and within a year, X-rays were being used in medical imaging, diagnosis and therapy. Also in the dental community, the importance of X-rays was recognized. Only 14 days after Roentgen published his discovery, Dr. Otto Walkhoff, a dentist in Braunschweig, Germany, produced the first images of his teeth with an exposure time of 25 minutes (5, 6).

Since then, dental imaging has undergone a major evolution due to the technological advancements that were made. The change from analogue to digital radiography has made the process much faster and simpler. Furthermore, the invention of computed tomography (CT) in 1975 by Sir Godfrey N. Hounsfield and Allan McLeod Cormack resulted in the replacement of 2D-images by 3D-images (5). However, the use of CT for dental imaging remained limited until the development of dedicated cone beam CT scanners for the oral and maxillofacial (OMF) region in the late 1990’s. These dedicated CBCT scanners were pioneered by Arai *et al.* in Japan (7) and Mozzo *et al.* in Italy (8). The first CBCT unit for dental use was approved by the FDA for the US market in March 2001. During the last few years, dental CBCT has become an integral part of the diagnostic toolset for several dental specialities (9).

1.3 Dental cone beam computed tomography

Dental CBCT is an innovative medical imaging technique that uses a cone-shaped beam of X-rays to generate three-dimensional (3D) images of the OMF region. The technique has become widely available and has found applications in different specialized fields of dentistry including orthodontics, endodontics, implant dentistry and maxillofacial surgery (10, 11). By using a cone-shaped beam of X-rays, rather than a fan-shaped beam, accurate 3D-images can be reconstructed after a single rotation of the X-ray source. This reduces the exposure time for the patient. The great benefit of this technique is that it can improve diagnosis, treatment planning and follow-up by providing these accurate 3D-images rather than the classical 2D-images provided by conventional radiography (see Supplementary figure 2) (9).

1.3.1 Radiation doses

Various dose units have been defined to describe medical radiation doses. The ones most frequently used are the absorbed dose, the effective dose, and the equivalent dose. The *absorbed dose* is the amount of energy that is delivered per mass of tissue that is exposed. This unit is usually expressed in Gray (Gy) (1 Gy = 1.0 Joule/kg) and is used to measure the output of an X-ray source, as for example a CBCT-scanner (10, 12).

For radiation protection purposes, the effective dose and equivalent dose have been defined. The *effective dose* is the most commonly used measure to describe the potential biological risk associated with exposure to IR in humans. It is a calculated unit which considers the radiation-sensitivity of the various tissues by using a tissue-specific weighting factor. The *equivalent dose* takes into account that different radiation qualities (i.e. photons, neutrons, protons, α -particles, etc.) have different biological effects on tissue for the same amount of energy deposited, by using a radiation-dependent weighting factor. These weighting factors are defined and re-evaluated by ICRP (latest revision in 2007) (13). Both the equivalent and effective dose are expressed in Sievert (Sv) (1 Sv = 1.0 Joule/kg).

1.3.2 Radiation doses associated with dental CBCT

In 2010, The New York Times newspaper published an article entitled: "Radiation worries for children in dentist's chair" (14). This article brought concerns about patient radiation doses in dental CBCT to the broader public. Especially in orthodontics, a large portion of dental X-ray procedures is performed on children, who are in general more sensitive to radiation than adults (9). In dental CBCT a wide range of doses is observed ranging from 13-1073 μ Sv (3, 13, 15, 16). These doses overlap with doses observed in multi-slice CT (MSCT) (474-1160 μ Sv)(15) and panoramic radiography (3-24 μ Sv) (16). However, generally the radiation doses associated with dental CBCT are less than the doses used in MSCT, but they are still up to 45 times higher than the doses used in panoramic and intra-

oral imaging (see Supplementary table 1) (10, 17). For dental CBCT the delivered radiation dose strongly depends on the type of apparatus that is used and the scan parameters (tube potential (kV) and tube current-time product (mAs)) selected by the user. As the resolution or exposed volume (field of view, FOV) is increased, the resulting radiation dose will increase as well. Therefore, matching FOV and the resolution to the intended usage will help to minimize patient radiation doses (9). Furthermore, the easy accessibility, easy handling, low cost and small size of the available dental CBCT devices facilitates in-office imaging. This has caused a shift in the user group from radiologists towards dentists (9). This shift has strengthened the existing concerns since these dentists have less expertise on the different aspects involved in X-ray imaging.

1.4 Biological effects of ionizing radiation

Epidemiological studies on atomic bomb survivors in Japan have provided great insight into the biological effects of both low and high doses of IR on human health. It is known that IR damages the cells by interacting with biological structures such as the DNA, proteins and lipids, resulting in damage to these structures. X-rays are a form of electromagnetic radiation with an energy, high enough to overcome the binding energy of electrons orbiting atoms. Interaction of X-rays with these electrons results in the formation of ions, hence 'ionizing' radiation (18). IR can directly damage cellular structures or indirectly through the induction of free radicals like hydroxyl (OH) or hydrogen peroxide (H₂O₂) (see Supplementary figure 3). Since more than 60% of our body consists of water, this indirect mechanism, in which the interaction between X-rays and water molecules results in the formation of free radicals, is the most prevalent damage mechanism for X-ray exposure (12, 18, 19). For this thesis, the focus will be on IR (i.e. X-rays) induced oxidative stress and the consequent effects on the DNA.

1.4.1 Oxidative stress after ionizing radiation

IR-induced oxidative stress results from the imbalance between reactive oxygen species (ROS) and the antioxidant defence mechanisms in the body. Free radicals induce oxidative damage to cellular structures, which can result in serious pathophysiological consequences. This radiation-induced oxidative stress does not only occur in the irradiated cells but also in their neighbouring cells. Moreover, oxidative damage may continue to rise for days and even months after the initial exposure presumably because of continuous generation of ROS (20).

Given the highly reactive nature of free radicals and their short half-life, it is preferred to measure the products that are formed during the reaction of ROS with cellular structures rather than measuring free radicals themselves (21). 8-hydroxy-2'-deoxyguanosine (8-OHdG) is an oxidized form of the guanosine base, resulting from oxidative stress. Upon DNA repair, 8-OHdG is excreted in the bodily fluids such as saliva. Therefore, 8-OHdG is a direct marker of oxidative stress-induced DNA

damage, which can be measured in saliva. However, it was reported that the measured levels of 8-OHdG do not only reflect the true oxidative DNA damage but also reflects dGTP present in the DNA precursor pool (21). In our study, saliva was chosen as sample medium to measure the level of 8-OHdG due to its availability, easy non-invasive collection, and the possibility of repeated sampling. Because of these properties saliva is an interesting alternative to blood samples for screening and diagnostic applications (21).

1.4.2 Types of DNA damage after ionizing radiation

As mentioned earlier, IR can damage cellular macromolecules such as DNA. IR can cause different types of DNA lesions. The most important ones are single strand breaks (SSBs), double strand breaks (DSBs) and base alterations. However, cross-links between two DNA molecules or between a DNA molecule and a protein can also occur but are less frequent (18, 19). The DNA DSBs are considered the most harmful lesion type, because they are less likely to be repaired correctly (12, 22). Consequently, insufficient or inaccurate repair of these DNA DSBs can result in mutations, chromosomal translocation, apoptosis and/or carcinogenesis. It was estimated that each Gy of radiation induces 100,000 ionizations responsible for approximately 1000 base damages, 1000 SSBs and 20-40 DSBs. Despite this great number of ionizations, exposure to 1 Gy of radiation results in the mortality of only 30% of mammalian cells due to effective DNA repair mechanisms, especially for non-DSB lesions. The extent of the DNA damage depends on two intrinsic factors: the antioxidant capacity and the DNA repair capacity. Fortunately, various antioxidant mechanisms, like glutathione and uric acid, which can prevent oxidation, are present in our body. However, measurement of individual antioxidants is time consuming and labour-intensive. Therefore, measurement of total antioxidant capacity is preferred. Furthermore, our cells have two complementary repair mechanisms that can deal with DNA DSBs: non-homologous end rejoining (NHEJ) and homologous recombination (HR) (18).

1.4.3 The role of γ H2AX and 53BP1 in DNA damage response

Following DNA damage, our cells will respond by activating the so-called DNA damage response (DDR) which is responsible for recognizing and processing the DNA damage (23). The DDR is initiated by the MRE11–RAD50–NBS1 protein complex (MRN) which senses the presence of DSBs. Then ataxia-telangiectasia mutated (ATM) kinase is activated and phosphorylates H2AX, a variant of the core histone H2A family, at serine 139, creating γ H2AX at the DSB site (19). This γ H2AX was first observed in cells exposed to γ -rays hence its name (24). In turn, γ H2AX initiates a sequence of signalling events including the recruitment of p53-binding protein 1 (53BP1) (18, 23). 53BP1 is an important mediator in the DDR which is recruited to the DSB site to promote DSB repair. This protein is responsible for the recruitment of additional DSB responsive proteins and directs the DSB repair

process by determining the DSB repair pathway choice. 53BP1 is a promotor of the non-homologous end rejoining (NHEJ) repair mechanism (22). Both 53BP1 and γ H2AX form foci in the vicinity of DSBs which can be visualized.

Sedelnikova *et al.* have provided evidence on the quantitative relationship between the number of γ H2AX foci and the number of DSBs present (25), supporting the detection of γ H2AX foci as a reliable and sensitive monitor for DSB formation and repair (19). γ H2AX can be detected after only a few minutes in cells exposed to IR and phosphorylation reaches a peak at about 30 minutes post-irradiation (p.i.) (23). However, γ H2AX artefact foci can occur in the absence of DSBs, for example during S-phase replication fork stalling (26). Therefore, using a double immunocytochemical staining for both γ H2AX and 53BP1 can enhance the sensitivity of the assay, since radiation induced γ H2AX foci co-localize very reliably with 53BP1 foci (27). Therefore, to determine the DNA damage and repair kinetics after IR exposure, visualizing γ H2AX and 53BP1 co-localized foci over a 24 hour timeframe provides a powerful tool for monitoring the induction and repair of DSBs, since the disappearance of γ H2AX and 53BP1 foci matches DNA DSB repair (28).

1.5 Importance of radiation protection

As mentioned before, medical radiation exposure is the largest controllable radiation source in the world. Worldwide the number of medical procedures utilizing IR is increasing (29). This increase has raised concern since it is widely known that exposure to IR results in a wide array of health effects, including stochastic effects like carcinogenesis or deterministic effects like cataract (30). To control and limit these risks the following principles of radiation protection have been defined, in the context of diagnostic imaging.

- **Justification**

Justification implies that the procedure should only be performed if the use provides more benefit to the patient than harm. This means that the dental CBCT operator should carefully consider the necessity of the imaging procedure. Therefore, dental CBCT should only be performed when it is favourable over conventional 2D-dental imaging (10, 29).

- **Optimization**

Optimization focuses on minimizing radiation-induced risks by reducing the exposure following the ALARA-principle (As Low As Reasonably Achievable). This means that the applied dose has to be balanced against the imaging quality that is required for the intended outcome of the application (29). For dental CBCT, this can be achieved by selecting the appropriate imaging setting on an individual patient based level.

1.5.1 Radiation protection in children

When radiographing children, it is even more critical to follow these principles since children are more sensitive to radiation exposure than adults. The main reason for this difference in radiation sensitivity is the different differentiation status (actively dividing tissues vs. more differentiated tissues) in children and adults. Furthermore, because of their longer life expectancy children have a greater chance of developing radiation-induced cancer (31). It is estimated that the radiation risk for paediatric patients is approximately twice as high as for adults (10). In Belgium, the “Hoge Gezondheidsraad” has provided guidelines on the use of dental CBCT. However, these guidelines pay no special attention to the application of dental CBCT in paediatrics. To optimally implement the principles of radiation protection in practice, detailed knowledge of the biological effects and risks of IR is required (10).

1.6 Low dose radiation hypothesis

Radiation exposure and its associated risks and consequent health effects have been the subject of much research and debate. Little question exists that intermediate and high doses of ionizing radiation result in deleterious effects in humans including cancer induction. However, for low dose (<100 mGy) radiation exposure the situation is less clear. Despite previous studies on the topic, there is still much uncertainty about the dose-response relationship and the biological effects of low dose radiation (Figure 2). Generally, it is assumed that low dose radiation exhibits a linear-no-threshold (LNT) dose-response. In this model, even the lowest radiation dose will result in damaging effects and the biological response at low doses can be estimated by extrapolation from medium and higher doses. Most researchers support this LNT model, however, some alternative models suggest a deviation from this LNT model. In the threshold model, radiation exposure must exceed a threshold dose in order to initiate a response. Below this threshold no effects are observed. The hyposensitivity or hormetic model suggests that low dose radiation induces several beneficial cellular mechanisms, resulting in a protective effect on the cells. In contrast, the hypersensitivity model suggests an increased response resulting in greater biological damage, causing increased radiation sensitivity at low doses (32). Thus far, evidence explaining the dose-response relationship at low doses has been inconclusive. Therefore, research characterising the biological dose-response after low dose radiation exposure is required to support one of these models.

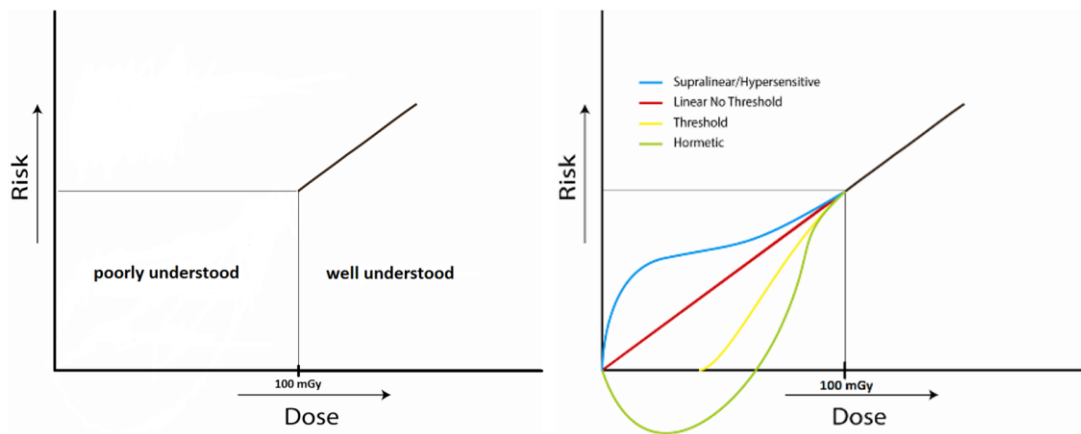


Figure 2: Graphical representation of the different models explaining the dose-response relationship within the low dose range (<100 mGy).

The linear-no-threshold model (red), the threshold model (yellow), the hyposensitivity/hormetic model (green) and the hypersensitivity model (blue) are illustrated (32).

1.7 Preliminary data

Preliminary data obtained at the Radiobiology Unit of SCK•CEN (Figure 3) show that the initial number of radiation-induced DNA DSBs in paediatric dental follicle stem cells (DFSCs) *in vitro* is restored to control levels after 24 hrs. After irradiation with low doses (5, 10, 20, 50 and 100 mGy), microscopic analysis showed that DNA DSBs are present in DFSCs, indicated by both γ H2AX (Fig. 3A) and 53BP1 foci (Fig. 3B), with a peak response 30 minutes after irradiation. After 24 hrs, the number of γ H2AX and 53BP1 foci decreased to control levels for all radiation doses. 4 hrs post irradiation, the lowest doses (5, 10 and 20mGy) show an unexpected peak of γ H2AX foci. Repetition of these experiments with a larger sample size should clarify whether this observation is a true response or due to an artefact in these results (*unpublished data*).

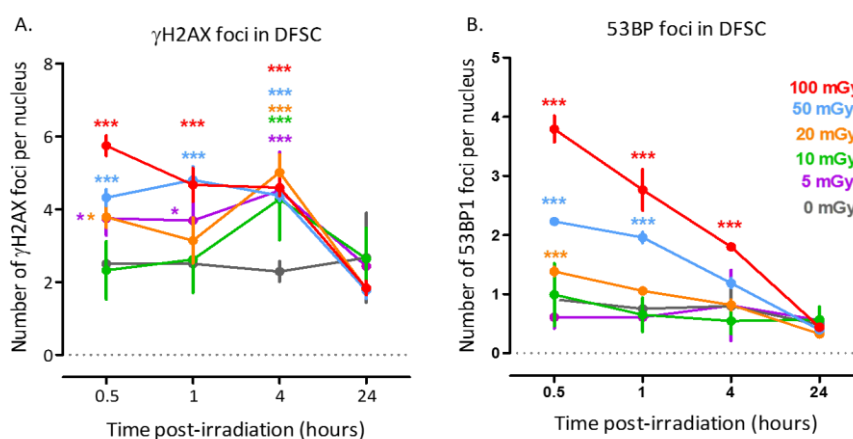


Figure 3: γ H2AX and 53BP1 repair kinetics after low dose X-irradiation (*in vitro*).

DNA DSB induction and repair kinetics was based on the number of γ H2AX and 53BP1 foci per nucleus measured 0.5 hour, 1 hour, 4 hrs and 24 hrs after low dose X-ray exposure (0, 5, 10, 20, 50 and 100 mGy) in DFSC. **A:** Quantitative analysis of γ H2AX foci. *: $P < 0.05$; **: $P < 0.01$ and ***: $P < 0.001$ compared to 0 mGy. **B:** Quantitative analysis of 53BP1 foci. ***: $P < 0.001$ compared to 0 mGy. Data were analysed with a 2 way ANOVA. DSB = double strand break, DFSC = dental follicle stem cells.

1.8 Experimental approach

This study aims to characterize the potential biological changes induced by dental CBCT imaging. More specifically, we will focus on DNA damage and oxidative stress levels after low dose X-ray exposure. We hypothesise that low dose radiation, as used in dental CBCT, induces more DNA damage and oxidative stress in the orofacial region in paediatric patients than in adults. To test this hypothesis, three objectives were defined:

1) Determine the dose response of low dose X-ray exposure (0, 5, 10, 20, 50, 100 mGy) on dental stem cells obtained from paediatric patients.

To test this first objective, *in vitro* radiation experiments will be performed on dental pulp stem cells (DPSC), dental follicle stem cells (DFSC) and stem cells of the apical papilla (SCAP). The three different stem cell types will be exposed to low dose (0, 5, 10, 20, 50, 100 mGy) radiation. Next, DNA damage and repair kinetics will be analysed by determining the presence of DNA DSBs by visualising γ H2AX and 53BP1 foci with fluorescence microscopy at multiple time points (30 min, 1 h, 4 hrs, and 24 hrs) p.i.. Only co-localized γ H2AX/53BP1 foci will be considered as DSBs. Additionally, the level of 8-OHdG and the total antioxidant capacity will be determined in the supernatant of the dental stem cells using an ELISA-assay and a FRAP-assay respectively. The oxidative stress level will be measured at the same time points as the DNA damage to enable correlation of the two biological parameters.

2) Determine the DNA damage response of clinical dental CBCT exposure on oral mucosa cells of paediatric patients and compare this with the response in adults.

To test this second objective, *ex vivo* experiments will be performed on exfoliated oral mucosa cells from paediatric patients. These cells will be collected immediately before dental CBCT exposure, 30 minutes after exposure and 24 hrs after exposure, using a buccal swab. The samples will be studied for DNA damage and repair kinetics by visualising the γ H2AX and 53BP1 co-localized foci. Adult samples will be included to identify potential age-dependent radiation sensitivity.

3) Pilot study: determine the feasibility of saliva profiling to detect dental CBCT-induced local changes in oxidative stress levels in the oropharyngeal region of paediatric patients and adults.

For this third objective, saliva samples will be collected immediately before and 30 minutes after dental CBCT exposure from paediatric patients. Next, the oxidative stress level of the samples will be determined by measuring the level of 8-OHdG and the total antioxidant capacity using an ELISA-assay and a FRAP-assay respectively. As with the buccal cells, adult saliva samples will be included to identify potential age-dependent radiation sensitivity.

2 Materials and methods

2.1 Participants

In this study both adults (>18 years old) and children (3-16 years old) were included. All participants submitted to dental CBCT were outpatients attending the department of dentomaxillofacial imaging, at the St-Raphael hospital (Leuven, Belgium), the Institutul Oncologic (Cluj-Napoca, Romania) or Hôpital Bichat-Claude-Bernard (Paris, France). Specifications of the dental CBCT units that were used in this study are provided in Table 2. Individual characteristics of the patients were collected including age, gender, allergies and previous imaging procedures during the last year. The study was approved by the ethical committee of KU Leuven, Comité d'Evaluation de l'Ethique des projets de Recherche Biomédicale (CEERB) Paris Nord and the Comisia de Etica U.M.F. Iuliu Hatieganu Cluj Napoca. Informed consent was obtained from all patients included in this study [adults n = 21, children n = 128]. For children (<18 years old), informed consent was signed by their parents.

Inclusion criteria

- Healthy children and adults referred for a dental CBCT scan by their doctor
- Children aged between 3-16 years old
- Good oral hygiene

Exclusion criteria

- Systemic disease or acute physical illness
- Use of antibiotics and anti-inflammatory drugs during the last 6 months
- Smoking

2.2 Sample collection of saliva and exfoliated oral mucosa cells

Saliva samples were collected immediately before and 30 minutes after dental CBCT using the passive drooling technique (Salimetrics®, Carlsbad, CA USA). Patients were asked not to eat, smoke or brush their teeth at least one hour before sampling and to rinse their mouth twice with water five minutes before each sample collection. Samples were stored at -20°C until they were sent to SCK•CEN. Upon arrival at SCK•CEN, saliva samples were stored at -80°C until further analysis.

Exfoliated oral mucosa cells were collected immediately before and 30 minutes after dental CBCT at the hospitals and 24 hrs after dental CBCT at the patients' home. Collection protocol was based on the protocol published by Thomas *et al.* (2009). Briefly, the cells were collected with the Catch-All™ Sample Collection Swab (Epicentre®, Madison, USA) by means of scraping of the buccal mucosa. This was performed on the inside of both cheeks using a different brush (for sampling left and right areas

of the mouth) to maximize cell sampling and to eliminate any unknown biases that may be caused by sampling only one cheek. After collection, the buccal cells were stored in 10 mL Saccomano's fixative (50% ethanol (VWR, Radnor, PA USA), 2% polyethylene glycol (Sigma-Aldrich chemistry, St-Louis, MO USA) which allows storage of the samples at 4°C up to 7 days. Cooled samples were then sent to SCK•CEN.

Table 2: Specifications of the dental CBCT units used in the different hospitals and the number of patients.

dental CBCT unit	Buccal cells		Saliva	
	Children (N)	Adults (N)	Children (N)	Adults (N)
<i>St-Raphael hospital (Leuven, Belgium)</i>				
Accuitomo kV = 90	21	1	21	1
Newtom kV = 110	29	20	29	20
<i>Hôpital Bichat-Claude-Bernard (Paris, France)</i>				
Planmeca Promax 3D Max. kV = 90	/	/	32	/
<i>Institutul Oncologic (Cluj Napoca, Romania)</i>				
NewTom 3G kV = 110	19	/	19	/
Planmeca Promax 3D Max kV = 90	24	/	24	/

2.2.1 Harvesting and fixation of exfoliated oral mucosa cells

Within 7 days after buccal cell collection (see 2.2 Sample collection of saliva and exfoliated oral mucosa cells), cells were harvested from the swab sample. The cell suspension was centrifuged for 10 min at 580g, supernatant was removed and the cell pellet was washed twice with buccal cell buffer (BuBu) (0.01M Tris-HCl (VWR, Radnor, PA USA), 0.1M EDTA (Sigma-Aldrich chemistry, St-Louis, MO USA), 0.02M NaCl (Merck, Billerica, MA USA), pH=7). The cell suspension was transferred to a new 15 mL tube. Afterwards, buccal cells were fixed in 2% paraformaldehyde (PFA) (Sigma Aldrich, St-Louis, MO USA) for 15 min at room temperature (RT). After fixation, buccal cells were stored at 4°C in 1x PBS until further analysis. Prior to immunostaining, the buccal cells were spotted onto Poly-L-lysine (Sigma-Aldrich, St-Louis, MO USA) coated coverslips using a cytocentrifuge (ThermoFisher Scientific, Waltham, MA USA). Afterwards, buccal cells were again fixed in 2% PFA for 10 min to ensure attachment of cells to the coverslip. Next, the buccal cells were stained (see 2.5.2 Immunocytochemistry for γ H2AX and 53BP1).

2.3 Cell cultures

2.3.1 Isolation and culture of paediatric dental stem cells

Dental pulp stem cells (DPSCs), stem cells of the apical papilla (SCAP) and dental follicle stem cells (DFSC) were isolated from three paediatric patients (courtesy of dr. Benjamin Salmon, Université Paris Descartes, France). The age and gender of the donors is presented in table 3. All cells were cultured in Dulbecco's Modified Eagle medium (DMEM, GIBCO, Life Technologies, Ghent, Belgium) containing 1 g/L glucose and pyruvate supplemented with 10 % fetal bovine serum (FBS) (GIBCO, Life Technologies, Ghent, Belgium). Cells were passaged at 70-80% confluence and the medium was changed every 2-3 days. Maximum passage number was P5 to limit/prevent spontaneous differentiation (33). Cell cultures were maintained in a humidified incubator (37°C; 5% CO₂). Cell cultures were tested for mycoplasma contamination using the Mycoplasma Detection Kit-QuickTest according to the manufacturer's protocol (Bimake, Munich, Germany, Cat °: B39032).

Table 3: Age and gender of dental stem cell donors.

	Age	Gender	DPSC	SCAP	DFSC
Donor 1	8	F	√	√	N.A.
Donor 2	12	M	√	√	√
Donor 3	11	M	√	√	√

2.3.2 Culture of PC3, A431, TICAE and Jurkat cells.

PC3, A431, TICAE and Jurkat cell lines were used as controls during a flow cytometry experiment to assess CK-4/CD45 expression on exfoliated oral mucosa cells. PC3 cells were cultured in Minimum Essential Medium (MEM) (GIBCO, Life Technologies, Ghent, Belgium) supplemented with 10% heat inactivated FBS (GIBCO, Life Technologies, Ghent, Belgium). A431 cells were cultured in DMEM (GIBCO, Life Technologies, Ghent, Belgium) supplemented with 10% heat inactivated FBS (GIBCO, Life Technologies, Ghent, Belgium). TICAE cells (courtesy of Dr. Ken Raj) were cultured in MesoEndo cell growth medium (Cell applications, CA USA) supplemented with 10% heat inactivated FBS. Finally, Jurkat cells were cultured in Roswell Park Memorial Institute medium (RPMI) (GIBCO, Life Technologies, Ghent, Belgium), supplemented with 10% heat inactivated FBS (GIBCO, Life Technologies, Ghent, Belgium). The medium was changed every 2-3 days and all cell cultures were maintained in a humidified incubator (37°C; 5% CO₂).

2.4 *In vitro* X-irradiation of dental pulp stem cells, stem cells of the apical papilla and dental follicle stem cells.

For irradiation purposes, DPSC, DFSC and SCAP were seeded into Lab-teks (8-well Sanbio, Uden, The Netherlands) 24 hrs before irradiation, to allow cells to properly attach, at a density of 25.000 cells/well. For all conditions six technical replicates were prepared. For the collection of supernatant after irradiation, the DPSC, DFSC and SCAP were seeded into 24-well plates (Greiner Bio-one,

Kremsmünster, Austria) at a density of 10.000 cells/well 24 hrs before irradiation. For all conditions three technical replicates were prepared.

X-irradiation experiments were performed at the irradiation facility available at SCK•CEN (Mol, Belgium). Cells were exposed to different doses of X-rays (0, 0.005, 0.01, 0.020, 0.050 and 0.100 Gy) with an Xstrahl 320 Kv tube using a vertical RX bundle with RQR-9 quality (120 kV, 1.8 mA, filtration with 2.9 mm Aluminium equivalent and 1 mm Copper) and a calculated dose rate of 0.9 Gy/h.

2.5 Analysis of DNA DSBs with γ H2AX and 53BP1 immunocytochemical staining

2.5.1 Fixation of dental stem cells and collection of supernatant

For immunocytochemistry purpose, DPSC, DFSC and SCAPs were fixed after irradiation at different time points (30 min, 1h, 4 hrs and 24 hrs). First, the supernatant was removed and the cells were washed twice with 1x PBS. Then the cells were fixed for 15 min with 2% PFA at RT and washed twice with 1x PBS. Stem cells were stored at 4°C in 1x PBS until further analysis.

For measurement of total antioxidant capacity and 8-OHdG, supernatant of DPSC, DFSC and SCAPs exposed to 0, 50 and 100 mGy was collected from 24-well plates at different time points p.i. (30 min, 1 h, 4 hrs and 24 hrs). After collection of supernatant, the cells were fixed for 15 min in 2% PFA at RT and stained with DAPI 1 μ g/mL for 1 h in the dark at RT. Cell count was based on DAPI signal to enable normalization of the data.

2.5.2 Immunocytochemistry for γ H2AX and 53BP1

After fixation, cells (buccal cells or stem cells) were washed three times with 1xPBS (Gibco, Life technologies, Ghent, Belgium) for 5 min. Next, the cells were permeabilized with 1x PBS-Triton X-100 0.25% (Sigma-Aldrich chemistry, St-Louis, MO, USA) for 3 min at RT. After 3 washes of 5 min in 1x PBS, cells were blocked with 1x pre-immunized goat serum (PIG) (ThermoFisher scientific, Waltham, MA USA) in a solution of 1x TBST, 0.005 g/v% TSA blocking powder (PerkinElmer, FP1012) (TNB) for 1h at RT. Next, cells were incubated with primary anti- γ H2AX antibody and anti-53BP1 antibody (see table 4) overnight on 4°C (buccal cells) or for 1h at 37°C (stem cells). Afterwards, the cells were washed three times in 1xPBS. Next an Alexa 488-conjugated goat anti-mouse antibody and an Alexa 568-conjugated goat anti-rabbit antibody (see table 4) were added. The cells were incubated for 1 h at 37°C in the dark. Afterwards, they were washed twice using 1x PBS. Finally, slides were mounted with ProLong Diamond antifade medium with DAPI (ThermoFisher Scientific, Waltham, MA USA). Samples were stored in the dark at -20°C until further microscopic analysis.

2.5.3 Fluorescence microscopy: γ H2AX and 53BP1 co-localized foci analysis

Images were acquired with a Nikon Eclipse Ti fluorescence microscope using a 40 \times dry objective (Nikon Tokyo, Japan). Images were analysed with Fiji software (34). The software allowed to analyse each nucleus based on the DAPI signal. Within each nucleus, intensity signal from the Alexa 488 and Alexa 568 fluorochromes were analysed after which the number of co-localized γ H2AX and 53BP1 foci per nucleus were determined in a fully automated manner using the Cellblocks tool (see Supplementary figure 4)(35).

2.6 Ferric Reducing Antioxidant Power (FRAP) assay

The OxiSelect™ FRAP Assay Kit (Cell Biolabs, CA USA) was used to determine the total antioxidant capacity of saliva samples and supernatant of dental stem cells. The FRAP-assay was performed according to the manufacturer's instructions. Briefly, a standard curve was created using Iron(II) standard stock solutions of 250 μ M, 125 μ M, 62.5 μ M, 31.3 μ M, 15.6 μ M, 7.8 μ M, 3.9 μ M and 0 μ M. Each standard and sample were analysed in triplicate. 100 μ l of each standard or sample and 100 μ l Reaction Reagent were added into a 96-well plate. Next, samples were mixed and incubated for 10 min at RT using a horizontal shaker. Finally, the absorbance was directly measured at 560 nm using a microplate reader (ClarioStar, BMG Labtech, Ortenberg, Germany). The results are expressed as Iron(II) concentration (μ M).

2.7 8-Hydroxy-2'-deoxyguanosine (8-OHdG) determination in saliva and supernatant

Before performing a competitive enzyme-linked immunosorbent assay (ELISA) the saliva samples were purified to reduce cross-reaction by uric acid etc.. Proteins and mucous substances were removed from the samples by filtering the samples and subsequently 8-OHdG was eluted. The saliva purification protocol for 8-OHdG was provided by the group of Dr. Siamak Haghdoost (University of Stockholm, Sweden)(36).

2.7.1 Purification of saliva and supernatant

First, saliva samples or supernatant were boiled for 5 min (90°C) and cooled down on ice for 10 min. Next 0.1% proteinase K (n° #EO0491, ThermoFisher Scientific, Waltham, MA USA) was added to the samples and then the samples were incubated for 60 min at 37°C. Next, the samples were again boiled for 5 min (90°C). Then they were cooled down on ice for 10 min and centrifuged for 30 min at 14000g at 4°C. After centrifugation the supernatant was transferred to a Microcon-30kDa Centrifugal Filter Unit with Ultracel-30 membrane (Merck, Billerica MA USA) and centrifuged for 60 min at 14000g at 4°C. The samples were kept on ice until further filtration steps.

2.7.2 Elution of 8-OHdG

For the elution of 8-OHdG, 500 µl phosphate buffer (pH=6.5) was added to 500 µl of the purified sample. Samples were kept on ice until they were loaded onto the columns. First, the vacuum columns were washed by applying methanol or MilliQ on the columns and by letting it run through completely. The following washing procedure was performed: methanol (1x), followed by MilliQ (2x), methanol (2x), MilliQ (2x) and methanol (2x). From this point on the columns were kept wet by closing the vacuum right before the fluid reaches the filter within the column. The columns were activated by applying methanol onto the column, then the columns were washed with solvent 1. Next, the purified samples were loaded onto the columns. Afterwards, the columns were washed with solvent 1 twice. Next, 130 µl of solvent 1A was loaded onto the column and run through the columns completely. Next 2 mL eppendorf tubes were placed under each column. Finally, 2 mL of solvent 2 was loaded onto the column, run through completely and the samples were collected in 2 mL eppendorf tubes. Collected samples were frozen and freeze-dried overnight. Finally, the columns were washed with MilliQ (1x), methanol (1x) and MilliQ (1x) before they could be used again. This entire procedure was performed twice. Freeze-dried samples can be stored at -20°C. After the first elution-round the freeze-dried sample were solved in 1 mL phosphate buffer (pH= 6.3) and kept on ice until the second filtration-round.

2.7.3 Enzyme linked immunosorbent assay (ELISA): 8-OHdG

The level of 8-OHdG was quantified using a competitive ELISA. The ELISA-kit and instructions were provided by Dr. Siamak Haghdoost (University of Stockholm). In summary, 270 µl of the purified saliva sample or supernatant was mixed with 165 µl primary antibody solution (80 ng/mL) and incubated for 2 hrs at 37°C. After incubation, samples were placed on ice for 10 min. Before loading the samples onto the ELISA plate, the plate was washed twice with 1xPBS. Next, 140 µl of the sample was loaded in triplicate onto the 8-OHdG-coated ELISA plate and incubated overnight at 4°C on a horizontal shaker. After incubation, the plate was washed three times with ELISA washing solution. Next, 140 µl of Horseradish peroxidase (HRP)-conjugated secondary antibody (diluted 1:2000) was added and the plate was incubated for 2 hrs at RT. After incubation, the plate was washed three times with ELISA washing solution and 1 time with 1xPBS. Finally, the reaction was visualized by the addition of 140 µl chromogenic substrate (3,3',5,5'-Tetramethylbenzidine (TMB+) (One-Step substrate system; Dako, Glostrup Municipality, Denmark) for 15 min in the dark. The reaction was stopped by adding 70 µl 2M H₂SO₄. The absorbance was measured at 450 nm (signal) and 570 nm (background) using a microplate reader (ClarioStar, BMG Labtech, Ortenberg, Germany). As a reference for quantification, a standard curve was established by a serial dilution of a 8-OHdG standard solution (0.01, 0.1, 0.5, 1, 3 and 10 ng/mL).

2.8 Analysis of buccal swab composition

2.8.1 Analysis of buccal swab composition using flow cytometry

Exfoliated buccal cells were identified with the epithelial marker cytokeratin-4 (CK-4) and CD45 was used as a marker for cells of lymphoid origin. A431 and PC3 (courtesy of Katrien Konings) cell lines were used as a positive control for CK-4 expression. TICAЕ (courtesy of Ken Raj) and SCAPs were used as a negative control for CK-4 expression. JURKAT cells were used as a positive control for CD45 expression. All cells were washed with 1x PBS and fixed in 70% ethanol (-20°C) at a concentration of 1×10^6 cells/mL or 2×10^6 cells/mL (JURKAT). Next, cells were washed once with a solution of 1x PBS, 5% FBS (GIBCO, Life Technologies, Ghent, Belgium) and 0.25% Triton X-100 (Sigma-Aldrich chemistry, St-Louis, MO USA) (PFT) and then blocked for 1h at RT in PFT. After blocking, cells were incubated with a rabbit monoclonal anti-cytokeratin 4 antibody (see table 4) overnight at 4°C on a horizontal shaker. Next, cells were washed twice with PFT. Subsequently, Alexa 488-conjugated donkey anti-rabbit secondary antibody and primary mouse anti-human monoclonal CD45 antibody labelled with allophycocyanin (see table 4) were added and the cells were incubated for 2 hrs at RT in the dark. After incubation, the cells were washed twice with PFT and treated with 10 µg/mL of the DNA dye 7-AminoActinomycin D (7-AAD) for 15 min at RT. 7-AAD was used to distinguish cellular material from debris. Furthermore, it gives information about the current cell cycle phase of the samples. Finally, the samples were filtered on a round bottom tube with cell-strainer cap (n° 352235 Falcon®, Corning, NY USA) and analysed on the BD Accuri™ C6 Flow Cytometer (BD Biosciences, San Jose, CA USA). At least 10.000 events were measured. Single-colour stained cells were included for colour compensation. Gating was based on PC3, A431, TICAЕ, Jurkat and SCAP cells that were used as positive/negative control for CK-4 or CD45.

2.8.2 Giemsa staining of buccal swab

To perform a Giemsa staining oral mucosa cells were collected according to the buccal cell collection method described in section 2.2.1 “Harvesting and fixation of exfoliated oral mucosa cells”. After fixation in 2% PFA cells were spotted onto poly-L-lysine coated coverslips. Next, cell were stained with Giemsa (1:50 in 0.2M acetate buffer pH = 3.36) (VWR international, Radnor PA USA) for 1h. After incubation cells were washed twice with milliQ and slides were mounted with DPX (VWR international, Radnor PA USA). Images were made with a Nikon Eclipse Ti brightfield microscope using a 20× objective (Nikon, Tokyo, Japan).

2.9 Statistical analysis

The statistical analysis was performed using Graphpad prism 7 (GraphPad Inc., CA USA). P values lower than 0.05 were considered statistically significant. 2-Way ANOVA and linear regression were used to analyse the DNA DSB induction and repair kinetics of DPSC, DFSC and SCAP after *in vitro* low dose radiation exposure. Repeated measures ANOVA was used to compare the number of γ H2AX and 53BP1 co-localized foci in exfoliated oral mucosa cells of children and a Friedman test was used to analyse adult data. Background level comparison between children and adults of DNA DSBs and radiation sensitivity between children and adults was analysed with a non-parametric Mann Whitney test. The salivary total antioxidant capacity and 8-OHdG concentration were analysed with a paired t-test. Background level comparison between children and adults of salivary 8-OHdG was analysed with an unpaired t-test with Welch's correction. Radiation sensitivity between children and adults in 8-OHdG formation was analysed with an unpaired t-test on log transformed data. TAC baseline measured before 12 p.m. and after 12 p.m. was analysed with an unpaired t-test with Welch's correction (children) and Mann Whitney test (adults). TAC of girls before and after 12 p.m. was analysed with a paired t-test and TAC of boys before and after 12 p.m. was analysed with a non-parametric Wilcoxon signed-rank test.

Table 4: Overview of the used antibodies.

Antigen	Host	Dilution	Manufacturer	Catalogue n°
Immunocytochemistry (buccal cells and stem cells)				
Primary Antibodies				
γH2AX	Mouse monoclonal Ab	1:300 in TNB	Merck Millipore	05-636
53BP1	Rabbit polyclonal Ab	1:1000 in TNB	Novus Biologicals	NB100-304
Secondary Antibodies				
GAM488	Goat anti-mouse Alexa Fluor® 488 (green-labelled)	1:300 in TNB	Life Technologies	A11001
GAR568	Goat anti-rabbit Alexa Fluor® 568 (red-labelled)	1:1000 in TNB	Life Technologies	A11011
Flow cytometry				
Primary Antibodies				
CK-4	Rabbit monoclonal Ab	1:100 PFT	Abcam	ab51599
CD45	Mouse monoclonal Ab	1:50 PFT	BD Biosciences	555485
Secondary Antibodies				
DAR488	Donkey anti-rabbit Alexa Fluor® 488 (green-labelled)	1:200 PFT	Life Technologies	A21206

3 Results

3.1 Biological response of paediatric dental stem cells after low dose *in vitro* radiation exposure

To investigate the effect of low dose radiation exposure on paediatric dental stem cells the induction and repair kinetics of DNA DSBs and oxidative stress level of the supernatant were analysed.

3.1.1 DNA DSB induction and repair after X-ray exposure in dental stem cells.

The induction and repair of DNA DSBs was evaluated with a double immunocytochemical staining of γ H2AX and 53BP1. Since γ H2AX and 53BP1 form foci in the vicinity of DSBs, as part of the DDR, microscopic visualization of these co-localized foci provide a reliable and sensitive tool to monitor DSBs (Figure 4A). The number of co-localized foci was determined after X-ray exposure to 0, 5, 10, 20, 50 and 100 mGy in DPSC, DFSC and SCAP, isolated from paediatric patients, at multiple time points (0, 0.5 h, 1 h, 4 hrs and 24 hrs) p.i.. Representative images of the γ H2AX and 53BP1 double immunocytochemical staining of DPSC fixed 0.5 h and 24 hrs p.i. are shown in Figure 4B.

In general, the number of co-localized foci increased with the dose. Typically, a peak response was observed 0.5 - 1h p.i., after which the amount of DSBs continuously decreased. After 24 hrs, the number of co-localized foci decreased to basal levels, indicating DNA DSB repair. These effects were observed in all dental stem cell types (DPSC, SCAP, DFSC) (Figure 4C-E). More specifically, in the DPSC exposure to 100 mGy induced significantly more γ H2AX and 53BP1 foci 30 min and 1 h p.i. compared to control cells (0 mGy) ($p < 0.0001$). A dose of 50 mGy also resulted in more co-localized foci 1 h p.i. compared to 0 mGy ($p = 0.0303$) (Figure 4C). In the SCAPs, the number of γ H2AX and 53BP1 foci, observed after exposure to 100 mGy, was significantly increased compared to 0 mGy 30 min, 1 h and 4 hrs p.i. ($p < 0.0001$, $p < 0.0001$, $p = 0.0267$ respectively). Furthermore, 50 mGy induced more foci 30 min and 1 h p.i. ($p = 0.0018$, $p = 0.0004$ respectively) and exposure to 20 mGy induced more foci 1 h p.i. ($p = 0.0416$) (Figure 4D). In the DFSC, significantly more γ H2AX and 53BP1 co-localized foci were observed 30 min, 1 h and 4 hrs after exposure to 100 mGy ($p < 0.0001$, $p < 0.0001$, $p = 0.0374$ resp.). 30 min and 1 h after exposure to 50 mGy and 30 min after exposure to 20 mGy the amount of co-localized foci was increased as well in DFSC ($p < 0.0001$, $p = 0.0015$, $p = 0.0030$ respectively) (Figure 4 E). Furthermore, linear regression plots of this data reveal a linear dose response 30 min, 1 h and 4 hrs p.i. (DPSC: $R^2 = 0.9730$, $R^2 = 0.9916$, $R^2 = 0.9639$; DFSC: $R^2 = 0.9938$, $R^2 = 0.9141$, $R^2 = 0.7540$; SCAP: $R^2 = 0.9798$, $R^2 = 0.9950$, $R^2 = 0.9444$) (Supplementary figure 5). Moreover, the slope decreased over time returning to a constant basal response 24 hrs p.i. (DPSC: $R^2 = 0.07794$, DFSC: $R^2 = 0.0130$ and SCAP: $R^2 = 0.4737$). No difference in radiation sensitivity was observed between the different dental stem cell types (Supplementary figure 5).

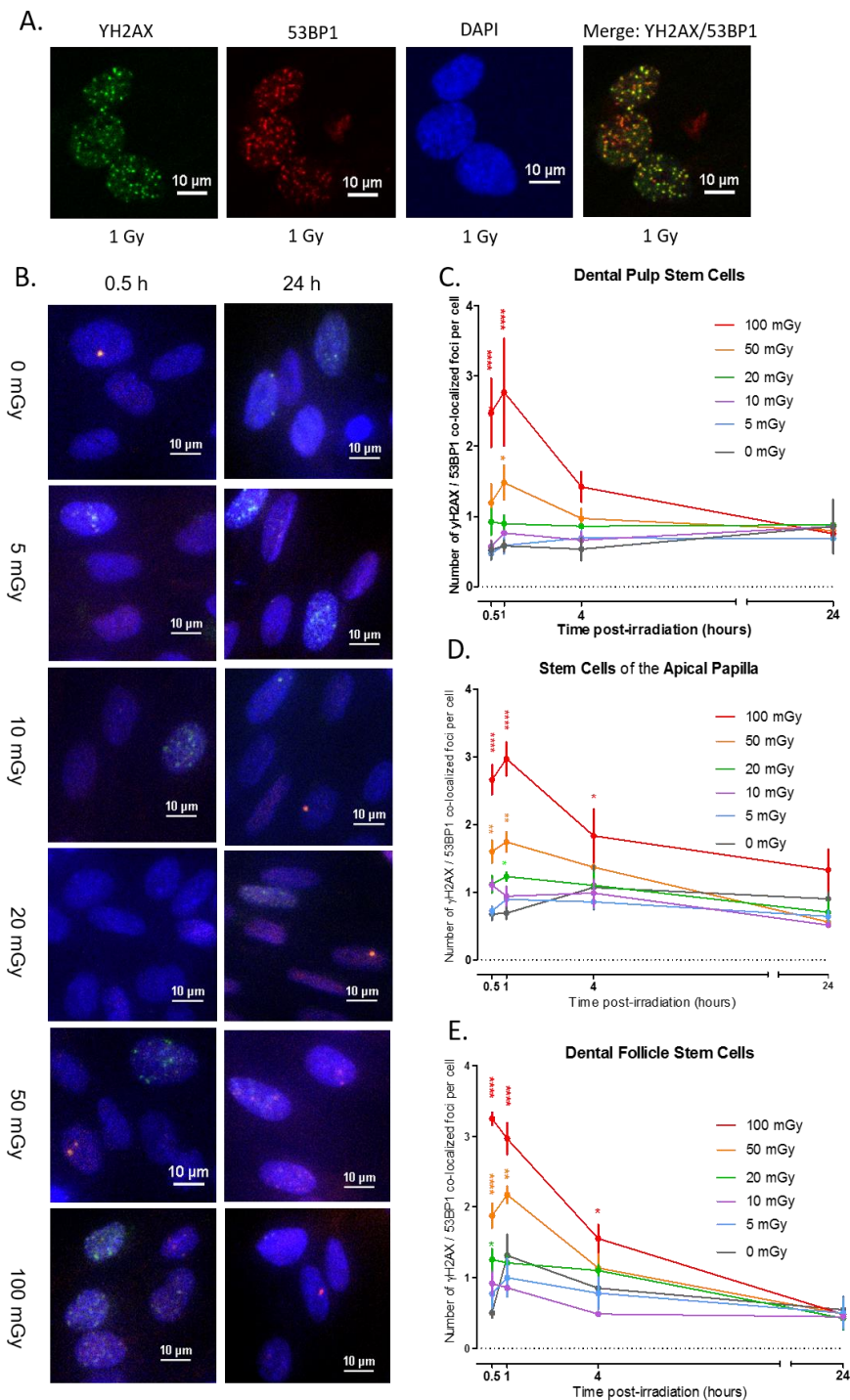


Figure 4: DNA DSB induction and repair after low dose X-ray exposure *in vitro* in dental stem cells.

DPSC, SCAP and DFSC, isolated from paediatric patients, were cultured and irradiated with low dose ionizing radiation (0, 5, 10, 20, 50 and 100 mGy). γ H2AX and 53BP1 double immunofluorescence staining was performed to quantify DNA double strand breaks. **A:** Immunofluorescence double-staining of γ H2AX (green) and 53BP1 (red) of DFSC after exposure to 1 Gy. DNA was counterstained with DAPI (blue). Images were merged to identify co-localized foci (yellow). **B:** Representative images of γ H2AX and 53BP1 immunofluorescence staining of DPSC fixed 0.5 h and 24 hrs after X-ray exposure. Note that the images show just cross-sections; for counting γ H2AX and 53BP1 foci, a z-scan covering the entire nucleus was performed. **C-E:** Quantitative analysis of the number of co-localized foci per cell measured 0.5 h, 1 h, 4 hrs and 24 hrs after X-ray exposure in DPSC (n = 3), SCAP (n = 3), and DFSC (n = 2) respectively. Data were analysed with a two-way ANOVA: *: <0.05, **: <0.01, ***: <0.001, ****: <0.0001. DPSC = dental pulp stem cells, DFSC = dental follicle stem cells, SCAP = stem cells of the apical papilla, DSB = double strand break.

3.1.2 8-OHdG in supernatant of dental stem cells after *in vitro* X-ray exposure using an ELISA-assay

8-OHdG was measured with a competitive ELISA-assay to assess the level of oxidative stress in dental stem cells (DPSC, DFSC and SCAP) after X-ray exposure. Supernatant of the dental stem cells was collected 30 min, 1 h, 4 hrs and 24 hrs after *in vitro* radiation exposure to 0, 50 and 100 mGy. Our first measurements, of the concentration of 8-OHdG in the supernatant of SCAP, were below the detection limit.

3.1.3 Total antioxidant capacity of supernatant of SCAP after *in vitro* X-ray exposure using a FRAP-assay

A Ferric reducing antioxidant power-assay (FRAP) was used to determine the total antioxidant capacity (TAC) of the supernatant of dental stem cells. SCAPs, DPSC and DFSC were exposed to a dose of 0, 50 and 100 mGy, and supernatant was collected 30 min, 1 h, 4 hrs and 24 hrs p.i.. So far, only SCAP samples were analysed. The TAC of supernatant of SCAPs ranged from 20 - 34 $\mu\text{M Fe}^{2+}$ (Figure 5). Since the cell culture medium contains pyruvate, which is a potent antioxidant, we decided to measure the TAC of both cell culture medium supplemented with 10% FBS and standard cell culture medium, as a control. In this way we could learn whether the TAC we measured in the samples was due to the secretion of the dental stem cells and not just the TAC of the cell culture medium itself. The TAC measured in the medium containing 10% FBS was the same as the TAC measured in the supernatant of SCAP cells (Figure 5A-B). The TAC measured in the standard cell culture medium was higher compared to the supplemented cell culture medium (Figure 5B). However, the observed difference was not statistically significant.

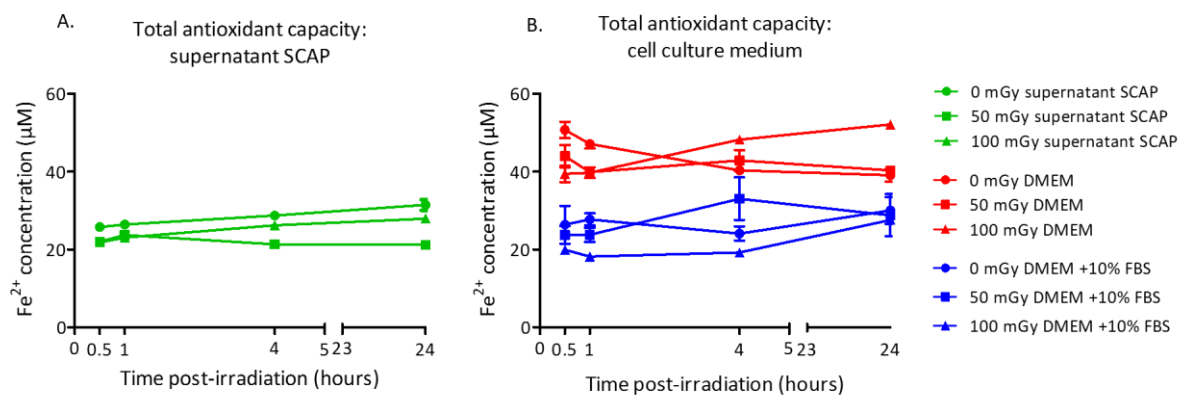


Figure 5: Total antioxidant capacity of supernatant of SCAP after low dose *in vitro* X-ray exposure.

The FRAP-assay was used to determine the TAC of the supernatant of dental stem cells exposed to IR. Supernatant of SCAPs exposed to 0, 50 and 100 mGy was collected 30 min, 1 h, 4 hrs and 24 hrs p.i.. (green). Cell culture medium (DMEM) (red) and cell culture medium (DMEM) supplemented with 10% FBS (blue) were used as controls. The TAC is determined via the reduction of Fe³⁺ to Fe²⁺ by antioxidants present within the samples and is expressed as Fe²⁺ concentration based on internal iron standard. The same level of TAC was measured in the supernatant of SCAP (blue) and in 10% FBS supplemented medium (blue). In the standard medium the level of TAC was higher. Data were analysed with a Mann Whitney test. TAC = total antioxidant capacity, FRAP = Ferric Reducing Antioxidant Power, FBS = Fetal bovine serum, SCAP = Stem Cells of the Apical Papilla, DMEM = Dulbecco's Modified Eagle Medium.

3.2 DNA double strand breaks in exfoliated oral mucosa cells after clinical dental CBCT exposure

To investigate the effect of dental CBCT on the DNA. We evaluated the induction of DNA DSBs. We were especially interested in these DSBs as they are less likely to be repaired correctly compared to SSB and thus pose a greater risk in cancer development. To investigate this, exfoliated oral mucosa cells were collected using buccal swabs.

3.2.1 Characterization of buccal swab composition using flow cytometry

First, the composition of the buccal swabs was characterized with flow cytometry in order to confirm that the cells, collected with our buccal swab collection protocol, were indeed exfoliated oral mucosa cells. Cytokeratin-4 (CK-4), an intracellular protein that is part of the cytoskeleton and which is specifically found in the differentiated layers of the mucosa, was used as a marker to identify exfoliated oral mucosa cells. Additionally, CD45, a membrane bound protein which is expressed on almost all haematopoietic cells, was used to screen for the presence of leukocytes within the buccal swab samples. Furthermore, 7-Aminoactinomycin D (7-AAD) was in this experiment used to stain the DNA. This enabled to distinguish cells from debris and to characterize the cell-cycle profile of the cells.

Flow cytometric analysis revealed that 97% of the cells, collected with a buccal swab, were indeed CK-4 positive (N=6) (Figure 6C). Only 1% of the cells was CD45 positive (Figure 6C). Figure 6D represent the results of one donor. For this donor 99.1% 7-AAD and CK-4 double positive cells were observed, which were identified as exfoliated oral mucosa cells. Furthermore, 7AAD-staining of the control cells (PC-3) clearly showed the different stages of the cell cycle ($G_{0/1}$ -phase, S-phase, $G_{2/M}$ -phase) (Figure 6E), whereas exfoliated oral mucosa cells did not show this profile, since they are fully differentiated (Figure 6F).

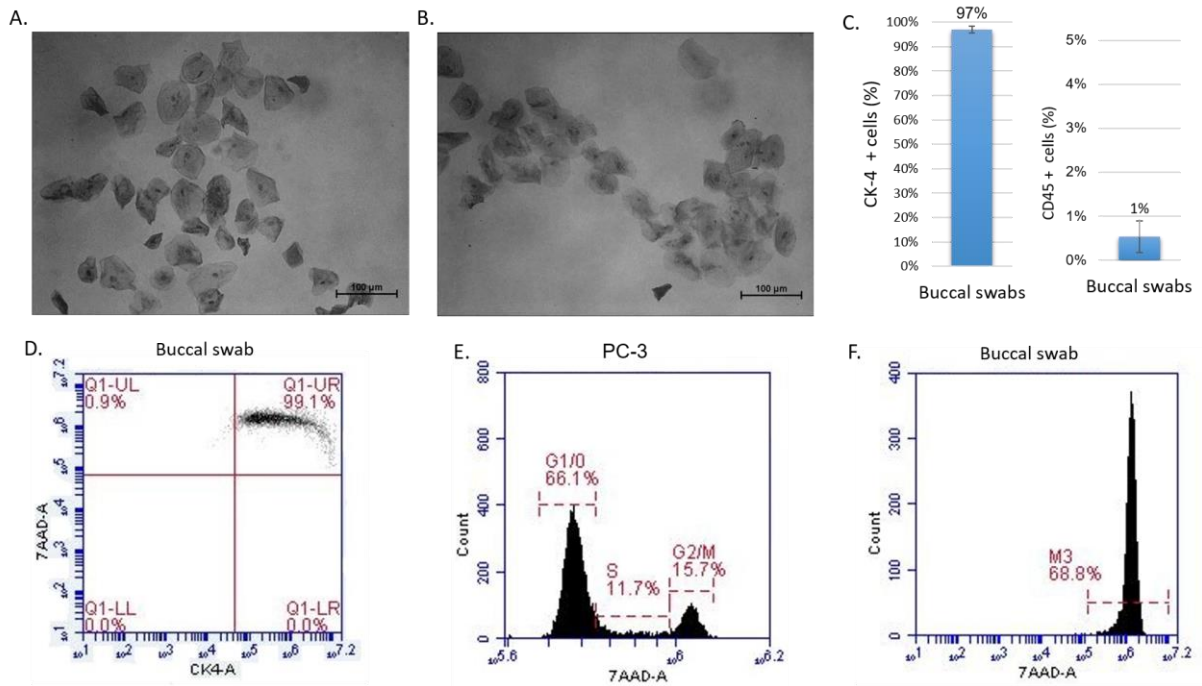


Figure 6: Flow cytometric characterization of buccal swab composition.

Buccal swabs were collected from six healthy individuals to analyse the composition of the swabs. Exfoliated oral mucosa cells present in the swabs were identified based on the expression of CK-4, the presence of leukocytes was determined based on the expression of CD45. 7-AAD staining was used to distinguish cells from debris and to generate a cell-cycle profile of the cells. **A-B:** Giemsa staining of exfoliated oral mucosa cells. **C:** 97% of cells present in the buccal swabs were identified as exfoliated oral mucosa cells and 1% as leukocytes (N= 6). **D:** Representative result of flow cytometric analysis of a buccal swab from one donor showed 99.1% 7-AAD and CK-4 double positive cells, which were identified as exfoliated oral mucosa cells. **E-F:** PC-3 cells were used as control culture and 7-AAD staining showed a clear G_{0/1}-phase, S-phase, G_{2/M}-phase profile, which was not observed in the buccal swabs. At least 10.000 events were measured. CK-4 = cytokeratin 4, 7-AAD = 7-Aminoactinomycin D.

3.2.2 DNA DSB induction in exfoliated oral mucosa cells after clinical dental CBCT exposure

In children, the average number of DNA DSBs increased from $0.2514 \pm 0,05$ co-localized foci/cell to 0.4679 ± 0.12 co-localized foci/cell 30 minutes after dental CBCT exposure. However, this increase was not statistically significant ($p = 0.0774$). Moreover, 24 hrs after dental CBCT the average number of DNA DSBs observed (0.2999 ± 0.09 co-localized foci/cell) did not differ from control levels measured before dental CBCT exposure (Figure 7). Also in adults, the number of DNA DSBs measured 30 minutes and 24 hrs after dental CBCT exposure did not differ significantly ($p = 0.6065$) from control levels (Figure 7). Furthermore, when we compared the basal level of DNA DSB occurrence between children and adults it was observed that the occurrence of DNA DSBs, in non-irradiated cells, was higher in children ($p = 0.0006$, Supplementary figure 6). Additionally, the radiation sensitivity of both groups (children and adults) was compared by analysing the response (Δ : after CBCT- before CBCT) between both groups. The response between children and adults did not differ ($p = 0.8268$, Supplementary figure 6). Finally, no difference in radiation sensitivity was observed between boys and girls (data not shown).

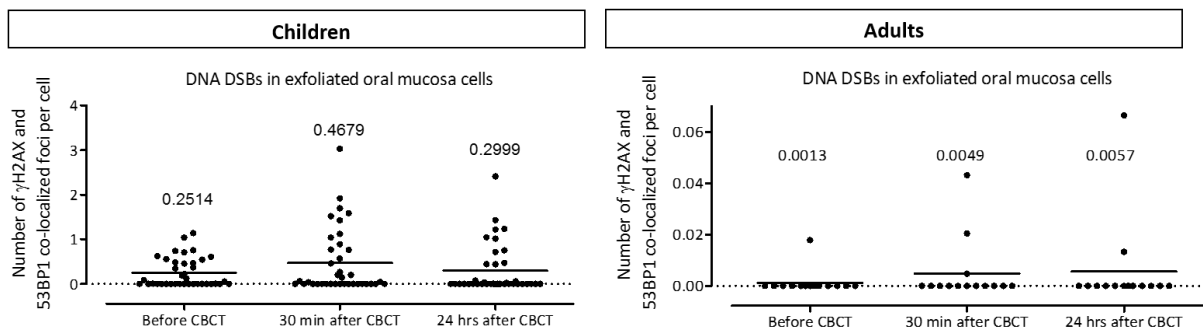


Figure 7: Number of DNA DSBs before and after dental CBCT exposure in exfoliated oral mucosa cells of children and adults.

Exfoliated oral mucosa cells were collected immediately before, 30 min after and 24 hrs after dental CBCT exposure from paediatric ($n = 37$) and adult ($n = 14$) patients. The mean number of γ H2AX and 53BP1 co-localized foci was determined with a double immunofluorescence staining. In both children and adults no statistical difference was observed ($p = 0.0774$, $p = 0.6065$ respectively). Data of the paediatric population was analysed with a Repeated measures one-way ANOVA and adult data was analysed with a Friedman test. DSB = double strand break, CBCT = cone beam computed tomography.

3.3 Measurement of oxidative stress in saliva after clinical dental CBCT exposure

To assess the level of oxidative stress induced by dental CBCT exposure 8-OHdG and TAC were determined in saliva of both children and adults.

3.3.1 Measurement of 8-OHdG concentration in saliva with an ELISA-assay

In children, a significant increase in 8-OHdG concentration was measured 30 minutes after dental CBCT exposure ($p = 0.0003$) (Figure 8). Moreover, before dental CBCT exposure an average value of 2.756 ± 0.48 ng/mL was observed and 30 minutes after dental CBCT an average value of 7.990 ± 1.14 ng/mL was observed. In adults, the mean concentration of 8-OHdG measured in saliva before dental CBCT examination (1.526 ± 0.36 ng/mL) did not significantly differ from the concentration measured 30 minutes after dental CBCT exposure (2.399 ± 0.59 ng/mL) ($p = 0.1973$) (Figure 8). Furthermore, the basal level of 8-OHdG, measured before dental CBCT, was higher in children than in adults ($p = 0.0416$; Supplementary figure 7). In addition, the radiation sensitivity was compared between children and adults and it was observed that the response in children was stronger than in adults ($p = 0.0004$, Supplementary figure 7). Furthermore, no gender differences were observed in children or adults (data not shown).

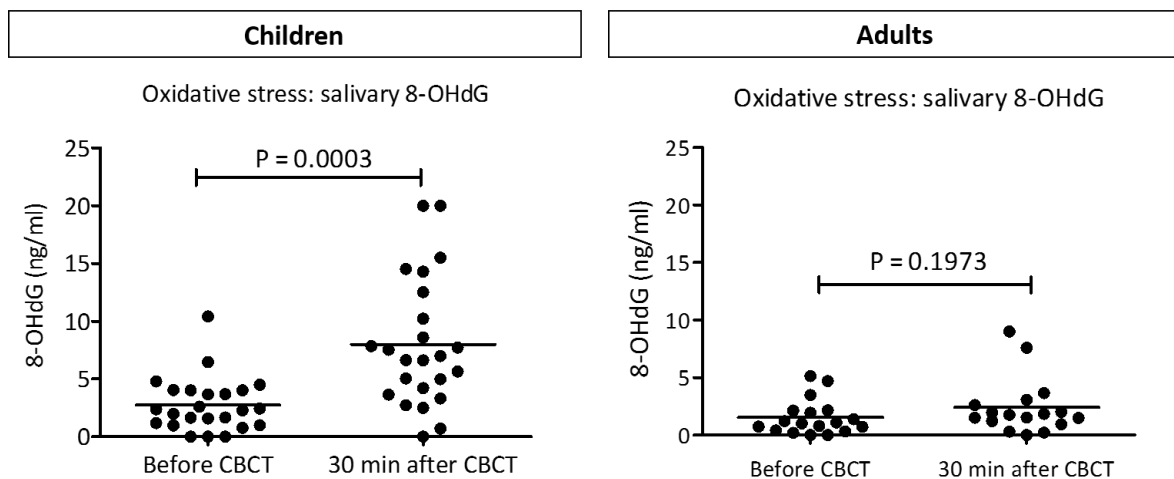


Figure 8: Salivary 8-OHdG concentration before and after clinical dental CBCT exposure in children and adults.

The salivary 8-OHdG concentration was determined with a competitive ELISA-assay. There was a significant increase in salivary 8-OHdG concentration in children ($n = 24$) after dental CBCT ($p = 0.0003$). In adults ($n = 16$), no significant difference in salivary 8-OHdG concentration was observed ($p = 0.1973$). Data were analysed with a Paired t-test. ELISA = Enzyme Linked Immunosorbent-assay, CBCT = cone beam computed tomography, 8-OHdG = 8-hydroxy-2'-deoxyguanosine.

3.3.2 Measurement of total antioxidant capacity of saliva after clinical dental CBCT exposure with a FRAP-assay

The level of oxidative stress after irradiation is determined by both the induction of reactive oxygen species and the antioxidant defence mechanisms present. Therefore, in combination with the previously described ELISA-assay, the total antioxidant capacity of the saliva samples was determined using a FRAP-assay.

The observed data show that there was an increase in the total antioxidant capacity of saliva samples from children collected after dental CBCT exposure ($p = 0.0282$). For adults on the other hand, a reduction of the total antioxidant capacity was observed after dental CBCT exposure ($p = 0.0412$). Furthermore, for both adults and children, we divided the patients into two groups based on the time of their CBCT examination (before 12 p.m. and after 12 p.m.). Then the basal level of TAC, measured before CBCT exposure, was compared between these two groups. Our data showed that the time of sampling (before 12 p.m. versus after 12 p.m.) affected the TAC, with higher levels measured in samples collected after 12 p.m.. Indeed, basal TAC measured in children after 12 p.m. was significantly higher than the levels measured in children before 12 p.m. ($p = 0.0217$) (see Supplementary figure 8A) and for adults, the same trend was observed. However, this effect was not significant ($p = 0.0893$) (Supplementary figure 8B).

Following these results, we further divided all patients based on the time of their appointment. Meta-analysis of these data revealed that, in both children and adults, TAC did not significantly differ after dental CBCT exposure (data not shown). Moreover, in both girls and boys who had their examination before 12 p.m. TAC was not altered ($p = 0.7394$, $p = 0.9658$ respectively) (see Supplementary figure 8C-D). For girls, who had their examination after 12 p.m. a significant increase in TAC was observed after dental CBCT exposure ($p = 0.0431$) (see Supplementary figure 8E). For boys, who had their examination after 12 p.m., no effect was observed ($p = 0.9382$, Supplementary figure 8F).

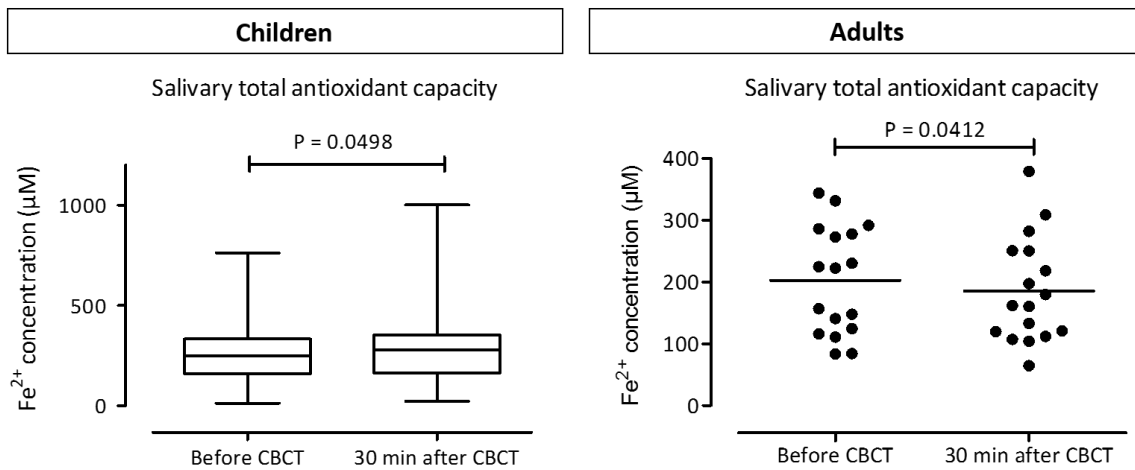


Figure 9: Total antioxidant capacity before and after clinical dental CBCT exposure in children and adults.

The FRAP-assay was used to determine the TAC of saliva samples that were collected before and 30 minutes after dental CBCT exposure. TAC is determined via the reduction of Fe³⁺ to Fe²⁺ by antioxidants present within the samples and is expressed as Fe²⁺ concentration based on internal iron standard. In children (n = 119), the TAC was increased after dental CBCT exposure (p = 0.0498). In adults (n = 17), the TAC was reduced after dental CBCT exposure (p = 0.0412). Data was analysed with a paired t-test. TAC = total antioxidant capacity, FRAP = Ferric Reducing Antioxidant Power, CBCT = cone beam computed tomography.

4 Discussion

Our research team at SCK•CEN investigated the response of DPSC, DFSC and SCAP to low dose IR exposure (*in vitro*) by analysing DNA DSB induction and repair and oxidative stress (8-OHdG and TAC). In addition, we analysed DNA DSB induction and repair in exfoliated oral mucosa cells and oxidative stress (8-OHdG and TAC) in saliva after dental CBCT examination (*ex vivo*).

4.1 Biological response of dental stem cells after low dose irradiation (*in vitro*)

Stem cells provide a source of self-renewing cells that can differentiate into specialized cell types. They are important in the process of development and repair as they can replace damaged cells. DPSC, for example, are vital for the maintenance of dentine and the dentine regeneration process in case of injury (37). When considering the use of dental CBCT in children, it is important to keep in mind that in children permanent teeth are developing and dental stem cells play a crucial role in this development. Therefore, knowledge on the impact of low dose IR on the different dental stem cell types (DPSC, DFSC and SCAP) is indispensable, as damage to the stem cell pool may result in developmental disturbances or poor recovery after injury. Moreover, malformations of the teeth, such as microdentia, delayed or arrested development of teeth and enlarged pulp chambers, were already observed in children exposed to high doses of IR during radiotherapy treatment of head- and neck cancer (38). To the best of our knowledge, the impact of low dose radiation on dental stem cells has not been investigated before. Therefore, the first objective of this study, was to characterize the biological dose response of low dose radiation exposure (0, 5, 10, 20, 50, 100 mGy) in DPSC, DFSC and SCAP obtained from paediatric patients.

4.1.1 DNA DSB induction and repair in dental stem cells after *in vitro* X-ray exposure

Our results demonstrate that low dose X-ray exposure (*in vitro*) results in the induction of DNA DSBs in DPSC, DFSC and SCAP, obtained from paediatric patients, in a dose-dependent manner. A peak response was observed 0.5 - 1 h p.i. after which the number of DNA DSBs gradually decreased to background levels, which were reached 24 hrs p.i.. Moreover, linear regression plots showed a linear increase in the number of DNA DSBs with increasing dose, 30 min, 1 h and 4 hrs p.i.. This effect was observed even for the lowest doses, although not statistically significant. Furthermore, the slope decreased over time returning to a constant basal response 24 hrs p.i.. These results suggest that most of the DNA DSBs, induced by low dose IR (<100 mGy), are repaired 24 hrs p.i. by DNA repair mechanisms (HR and HNEJ). Unfortunately, these repair mechanisms do not guarantee correct repair, posing a significant health risk as inaccurate repair of DSBs can still contribute to neoplastic transformation of cells. Moreover, in terms of carcinogenesis the consequences of radiation exposure are more severe in stem cells than in differentiated cells, due to their role as a long-term

reservoir for tissue regeneration and homeostasis (39). Ferguson *et al.* (2001) described a dual role for the HR and NHEJ DSB repair pathways in both prevention and creation of chromosomal translocation (40). NHEJ for example repairs DSBs by directly re-ligating DNA ends, which may result in gene deletions (40). It is important to consider the consequences of these gene deletions, especially since we monitor 53BP1 foci and 53BP1 is known to promote the NHEJ repair pathway (22).

Our results, observed in dental stem cells, support the linear no-threshold dose-response relationship. Although this is true for DNA damage (DSBs), it might be that for different parameters, like apoptosis or IR-induced premature senescence, and different cell types an alternative hypothesis applies. Previous research has already demonstrated that the radiation response of several tissue stem cells (i.e. skin, breast, brain and intestine) does not follow a unified model. For example, skin stem cells appear to be more resistant than their daughter cells whereas intestinal crypt stem cells are more sensitive than their progenitor cells (39, 41).

As a future perspective, it would be interesting to investigate additional biological end points like cell proliferation, cell cycle arrest, senescence and apoptosis. In this way, the observed effects on the DNA can be related to potential functional deficits. During cell cycle arrest, DNA damage is repaired. If the repair is unsuccessful, the cells are removed, mostly by apoptosis. However, in some cells this cell cycle arrest becomes permanent. These cells thus lose their proliferative potential, a condition known as premature senescence. Previously it was shown that DPSC exposed to IR (2-20 Gy) enter stress-induced premature senescence without affecting their viability (37, 42). Furthermore, it would be interesting to investigate the effect of IR on the differentiation potential of the stem cells since Havelek *et al.* (2013) showed that IR (6 Gy) initiates spontaneous odontogenic/osteogenic differentiation of DPSC resulting in a reduced amount of naïve DPSC, which may contribute to reduced recovery (37). The above described effects were observed at high doses of IR, however it is interesting to look further into these effects within the low dose range. Furthermore, linking back to our hypothesis, it would be interesting to compare the response of paediatric dental stem cells to the response in adult dental stem cells to identify age-related differences.

4.1.2 Total antioxidant capacity of supernatant of SCAP after *in vitro* X-ray exposure

Besides DNA damage and repair, we also characterized the level of oxidative stress in the supernatant of dental stem cells. Our findings demonstrate that the TAC measured, 30 min, 1 h, 4 hrs and 24 hrs p.i. in supernatant of SCAP, irradiated with 50 and 100 mGy, did not differ from the TAC measured in regular cell culture medium (DMEM containing 10% FBS), which was used to culture the SCAP cells. These results suggest that the TAC measured in the supernatant reflects the TAC of the cell culture medium itself and does not provide information on the excretion of oxidants by the irradiated SCAP cells. A possible explanation for this observation is that too little cells were

seeded or that the volume of cell culture medium was too high. Possible solutions to increase the concentration of excretion products in the supernatant is to seed more SCAP cells or to reduce the volume of cell culture medium on the cells. However, another alternative approach can be to measure the TAC of the cell lysate instead of the supernatant. In this way not only the excreted antioxidants but also the intracellular antioxidants can be measured. In addition, we measured the TAC of DMEM cell culture medium (with low-glucose). Surprisingly, our results showed that the TAC measured in the standard DMEM cell culture medium was higher (statistically not significant, $n = 3$) compared to the TAC measured in DMEM supplemented with 10% FBS. This observation suggests that the addition of FBS lowers the TAC of the cell culture medium. This finding is unexpected since the micronutrients that are present in FBS, like vitamins A, E and C and selenium, are known to have antioxidant activity (43). Repetition of the experiment is needed to further validate these results.

4.1.3 Concentration of 8-OHdG in supernatant of SCAP after X-ray exposure (*in vitro*)

The concentration of 8-OHdG measured in the supernatant of SCAP cells exposed to 0, 50 and 100 mGy was below the detection limit of the ELISA-assay. Upon DNA repair, 8-OHdG is excreted by the cells. Therefore, it should be possible to measure it in the supernatant. Because of time restraints we only analysed the supernatant of the SCAP cells. However, to get a complete picture the concentration of 8-OHdG in the supernatant of DPSC and DFSC should be analysed as well.

4.2 DNA damage in exfoliated oral mucosa cells of children and adults after dental CBCT exposure

4.2.1 Composition of buccal swabs

First, the composition of the buccal swabs was characterized to ensure that the cells, collected with our buccal swab collection protocol, were indeed exfoliated oral mucosa cells. Analysis of buccal swab composition of healthy volunteers demonstrated that 97% of cells present in the buccal swabs were CK-4+ (exfoliated oral mucosa cells) and 1% were CD45+ (leukocytes). These results are in line with previously published data from Metaxas *et al.* (2005). They analysed buccal swabs from 10 healthy volunteers and searched for the presence of CD45+ haematopoietic cells. In 6 out of 10 healthy volunteers CD45+ cells were detected (median 0.3%, range 0–1.5%) (44). Although we cannot rule out the presence of debris and bacteria in the sample, we are confident that these are excluded from the analysis through the gating process based on cell size.

4.2.2 DNA DSBs in exfoliated oral mucosa cells of children and adults after dental CBCT exposure

Our research group at SCK•CEN determined the DNA damage response in exfoliated oral mucosa cells of paediatric patients and adults, after clinical dental CBCT exposure. Our findings demonstrate that there is no statistically significant difference in the observed number of γ H2AX and 53BP1 co-localized foci before, 30 minutes after and 24 hrs after dental CBCT exposure in both children and

adults. Exfoliated oral mucosa cells have already been successfully used as biomarker for genotoxic effects resulting from occupational exposure, life-style factors, but also radiotherapy (45). The collection of these cells is rather easy and non-invasive. Furthermore, the oral mucosa cells are directly exposed to ionizing radiation during a dental CBCT examination, making them the ideal target cell to analyse DNA damage after dental CBCT examination.

Several studies assessed the genotoxic (micronucleus) and cytotoxic effects (pyknosis, karyolysis and karhyorrhexis) of dental radiography on exfoliated oral mucosa cells of both paediatric and adult patients. These studies all reported that micronucleus frequency before and after X-ray exposure did not differ significantly. Whereas, the number of other nuclear alterations, closely related to cellular death, such as pyknosis, karyolysis and karhyorrhexis, did increase significantly (46-49). These findings suggest that dental radiography does not induce genotoxic effects in exfoliated oral mucosa cells from paediatric patients and adults but can promote cytotoxicity. Conversely, Preethi *et al.* (2016) reported a significant increase in micronucleus frequency in exfoliated oral mucosa cells after bitewing and panoramic dental radiography in paediatric patients (45). Furthermore, Yoon *et al.* (2009) investigated γ H2AX expression in exfoliated oral mucosa cells of adults after dental radiography (2.34 cGy) exposure and showed a significant increase (50). It is noteworthy that comparing the results of biomonitoring studies of different populations exposed to different radiographic methods is quite difficult as each population is exposed to different radiation doses. This could explain why some studies find an increase in DNA damage, whereas others do not observe this.

Damage that leads to the formation of micronuclei takes place in the basal layer of the epithelial tissue, where cells undergo mitosis (47). For the micronucleus assay, buccal cells are best collected 10 days after X-ray exposure since rapid turnover brings these basal cells to the surface where they exfoliate 7-21 days later (46). Unfortunately, the micronucleus assay fails to provide information on the process of DNA DSB induction and repair kinetics. Therefore, we used the advanced γ H2AX and 53BP1 double immunocytochemical staining in our study. Since, the time window for detection of γ H2AX after IR exposure is ± 10 min - 48 hrs, buccal cells were collected 30 minutes and 24 hrs after dental CBCT exposure (23). This implies that, at the time of X-ray exposure, the cells that we collected were already present in the differentiated layers of the mucosa rather than the basal layer. Therefore, this detection method does not provide information on the processes going on in the basal cell layer of the mucosa. This is important to keep in mind as the sensitivity and DSB repair capacity may be different in basal cells and differentiated cells.

We observed 0.0046 ± 0.016 γ H2AX and 53BP1 co-localized foci/cell in non-irradiated adult buccal cells. This is lower than the foci rate reported by Gonzalez *et al.* (2010). They observed a γ H2AX foci rate per cell of 0.08 ± 0.02 in non-irradiated exfoliated oral mucosa cells of adults (51). This

difference might be explained by the enhanced sensitivity of the γ H2AX and 53BP1 double immunostaining. Since, this double immunostaining reduces the detection of γ H2AX artefact foci which can occur in the absence of DSBs during S-phase replication fork stalling (26). Furthermore, we noticed that the occurrence of γ H2AX and 53BP1 co-localized foci in non-irradiated cells was significantly higher in children (average value measured among 38 children : 0.2514 ± 0.05 foci/cell) than in adults (average value measured among 14 adults : 0.0013 ± 0.001 foci/cell). These findings are not in line with what one would expect. Since accumulation over time of DNA damage would result in higher levels of endogenous DNA damage in adults than in children. Ramsey *et al.* (1995) investigated the effect of age and life style factors on the accumulation of cytogenetic damage and showed a significant increase in stable aberrations (translocations and insertions) with age, supporting this idea (52). Moreover, a correct estimation of the endogenous DSB frequency is necessary to perform an accurate analysis of radiation induced DSBs as these endogenous DSBs provide a “noisy” background against which radiation induced DSBs have to be recognized. Moreover, since buccal cells are the first barrier in the inhalation and ingestion route they are exposed to different genotoxic agents. Therefore, inter-individual variation in the number of DNA DSBs in non-irradiated buccal cells, collected before CBCT exposure, may be explained by the influence of diverse environmental and life style factors such as diet, use of Listerine®, smoking etc. (45).

As children are said to be more radiation sensitive than adults, we compared the response between children and adults. Our findings demonstrated that the response did not significantly differ between children and adults, indicating, in contrast to what we hypothesized, that exfoliated oral mucosa cells of children do not exhibit an increased radiation sensitivity compared to exfoliated oral mucosa cells from adults. However, interpretation of these data requires caution as we did observe ± 0.23 more foci/cell in children after dental CBCT exposure. Ribeiro *et al.* performed a comparative analysis of the genotoxic and cytotoxic effects of dental radiography between children and adults demonstrating that there was no significant difference in micronucleus frequency or cytotoxicity (53). Their findings are in line with our data, although radiation doses used in conventional dental radiography are considerably lower than those used in dental CBCT.

4.3 Oxidative stress in saliva after dental CBCT exposure

As a last part of this study, we wanted to determine the feasibility of saliva profiling to detect local changes in oxidative stress in the oropharyngeal region of paediatric patients and adults after dental CBCT examination. When characterizing the biological response to IR and especially the effect on the DNA, it is important to realize that most of the DNA damage is not directly caused by IR, but rather indirectly from the free radicals that are created intracellularly by IR. Therefore, measuring oxidative stress is a valuable parameter in assessing the potential damaging effect after X-ray exposure. Saliva

was used as a collection medium, as it reflects the local environment. The last decade the interest in using saliva as a diagnostic fluid has increased due to the easy non-invasive collection method and the possibility of repeated sampling.

4.3.1 Salivary 8-OHdG concentration after dental CBCT exposure in children and adults

In this study, we have shown that the concentration of 8-OHdG measured in saliva of children was significantly increased after dental CBCT exposure. In adults, no significant increase in salivary 8-OHdG was observed. These results indicate that low dose IR involved in dental CBCT induces oxidative DNA damage in children, but not in adults.

Excreted levels of 8-OHdG depend on the cellular defence mechanisms. If the DNA repair capacity is reduced, 8-OHdG accumulates in the DNA and thus will not be excreted into the extracellular environment. This might explain why in adults, the concentration of extracellular 8-OHdG was not increased after dental CBCT, since an age-related decrease in DNA repair capacity was described before (54).

8-OHdG is a mutagenic lesion that can be formed in both mitochondrial and cellular DNA as well as in the nucleotide pool. However, the contribution of the nucleotide pool to excreted level of 8-OHdG is unclear. Sangsuwan *et al.* (2008) suggested that most of the extracellular 8-OHdG originates from this nucleotide pool, since they observed that hMTH1, a protein which inhibits the incorporation of 8-OHdGTP into the DNA by hydrolyzing 8-OHdGTP to 8-OHdGMP, was increased (55). However, oxidative DNA damage to the nucleotide pool also poses a risk for mutagenesis since 8-OHdGTP is a potent mutagenic substrate for DNA synthesis as the fidelity of DNA repair and synthesis is dependent on a balanced nucleotide pool (55).

Furthermore, background levels of 8-OHdG measured before dental CBCT exposure were significantly higher in children than in adults. Interestingly, the same observation was made for the background level of DSBs in exfoliated oral mucosa cells of children versus adults. Tamura *et al.* (2006) investigated age-related changes of urinary excretion of 8-OHdG and they observed a significant inverse correlation between age and urinary levels of 8-OHdG, with the highest levels observed in the youngest subjects (56). This observation supports our findings. In addition, they compared urinary 8-OHdG concentration between males and females and could not observe any significant differences (56). This is in line with our data, where no significant differences in salivary 8-OHdG between males/females or boys/girls were found.

In this pilot study saliva samples were collected 30 min after dental CBCT exposure. However, it is not sure whether this is the optimal time point to measure excreted levels of 8-OHdG post irradiation. For future experiments it would be interesting to include additional time points, i.e. 1 h, 3 hrs and 24 hrs p.i., to investigate the evolution of 8-OHdG concentration over time to determine the optimal time point for saliva collection post irradiation.

4.3.2 Total antioxidant capacity of saliva after clinical dental CBCT exposure

Finally, our findings demonstrate that dental CBCT exposure significantly increased the TAC measured in saliva from children, but significantly decreased the TAC in saliva from adults. However, in our study we found that the time of sampling (before 12 p.m. versus after 12 p.m.) significantly affected the TAC, with higher levels measured in samples collected after 12 p.m.. Kamodyova *et al.* (2015) already reported that FRAP levels varied during the day with the highest concentrations in the afternoon (57). Therefore, we divided all patients into two groups based on the time of their appointment. After this division, no significant differences in TAC before versus after dental CBCT were observed in both children and adults. These results suggest that dental CBCT examination does not influence TAC.

The use of TAC as salivary biomarker has already been investigated in relation to periodontal disease and dental caries (58). Decreased levels of TAC were associated with periodontal disease state (58). Previously, animal studies have shown that whole-body exposure to X-irradiation (0.5 - 3 Gy) decreased concentrations of ascorbic acid and vitamin E in bone marrow cells in a time-dependent manner (59). It has been reported that uric acid is the major antioxidant in saliva, contributing to more than 85% of the TAC (60). In addition, other antioxidants such as ascorbic acid, vitamins, albumin and antioxidant enzymes such as superoxide dismutase, catalase, and glutathione peroxidase all contribute to the salivary TAC (60, 61).

We measured an average FRAP value of $200.4 \pm 86.3 \mu\text{M Fe}^{2+}$ in saliva of adults before dental CBCT. This is lower than the values reported by Suma *et al.* (2010). They observed an average value of $610.83 \pm 4.52 \mu\text{M Fe}^{2+}$ in saliva of healthy controls, illustrating the high biological variability of salivary TAC. The use of saliva to measure TAC offers some challenges as various confounding factors were described to affect saliva composition (60). Besides, the circadian rhythm other confounding factors like gender, age and diet were described to affect salivary antioxidant status (57). However, our data did not reveal a significant difference between boys and girls or adults versus children.

In view of future research on this topic it is important to address in detail the study design hereby considering the influence of the previously described confounding factors. Furthermore, given the high biological variation it is evident that the number of patients has to be high to extract meaningful information. Nowadays different assays are available to measure the TAC including FRAP-assay, Trolox equivalent antioxidant capacity (TEAC) assay, total radical-trapping antioxidant parameter (TRAP) assay and the oxygen radical antioxidant capacity (ORAC) assay (62). The disadvantage of this wide choice of assays is that the results of these assays are expressed in different units which makes the comparison of results between the different assays impossible. Therefore, studies describing the correlation between these different assays would be very useful. Moreover, a systematic study of salivary total antioxidant capacity, providing reference values in healthy subject, is still lacking.

5 Conclusion

Dental CBCT is a low dose radiographic imaging technique that is frequently used in paediatric dentistry. To date, it remains unclear whether low dose radiation exposure is completely without risk. This question is especially important regarding children as they are known to be more sensitive to IR than adults. Therefore, the main goal of this research project was to investigate the potential biological effects (DNA damage and oxidative stress) induced by dental CBCT exposure. The focus was placed on children, but adults were also included to identify potential age-related differences.

Our *in vitro* results, observed in dental stem cells, support the linear no-threshold dose-response relationship in the low dose range (< 100 mGy) suggesting that even exposure to low doses of IR poses a risk. In contrast, our *ex vivo* results showed that dental CBCT exposure does not significantly induce DNA DSBs in exfoliated oral mucosa cells of children and adults. However, the amount of DNA DSBs measured before, 30 min p.i. and 24 hrs p.i. was significantly higher in children than in adults. In addition, we investigated the feasibility of saliva profiling to detect local changes in oxidative stress after dental CBCT exposure. We found that dental CBCT induces significantly more salivary 8-OHdG in children, but not in adults and that children exhibited a stronger response than adults, indicating that children are more sensitive to IR. Moreover, our results illustrate that subtle radiation-induced changes in 8-OHdG levels can be detected in saliva. Furthermore, we noticed that diurnal variations influenced the TAC of saliva. The easy non-invasive collection of saliva makes it a very interesting diagnostic fluid. However, numerous pitfalls should be taken into account, like diurnal variations and the high biological variation when assessing the TAC of saliva. Inclusion of additional patients, for example, will increase the reliability of the data.

Taken together we can conclude that further research is needed to get a complete understanding of the potential biological risks involved in dental CBCT exposure. Besides DNA damage and oxidative stress, other parameters like cell proliferation, cell cycle arrest, radiation-induced cellular senescence and apoptosis should be explored as well. Furthermore, it would be interesting to investigate the effect of repeated exposure as patients are often subjected to multiple procedures during treatment planning and follow-up. It might be interesting as well to include patients exposed to other imaging techniques including head CT.

The results of this study contribute to a better understanding of the biological effects induced by dental CBCT exposure in children and adults. In the end, this information will enable professional caretakers (dentists, medical radiologists, maxillofacial surgeons) to optimise the use of dental CBCT in their practice and will provide improved radiation protection to patients.

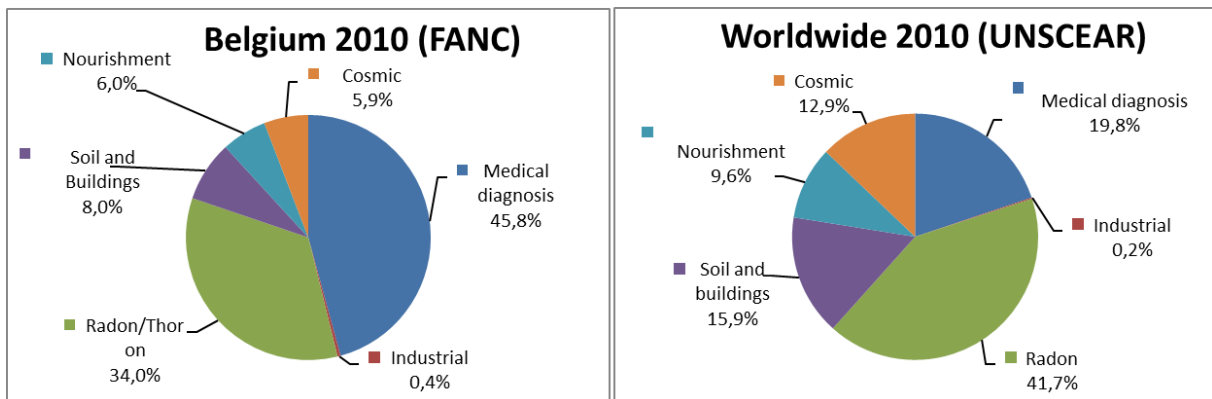
6 Literature references

1. Dr. Lionel Sombé JC, Michelle Bouchonville. Radiologisch toezicht in België Syntheseverslag 2014. FANC; 2014.
2. Organization WH. Communicating radiation risks in paediatric imaging: information to support health care discussions about benefit and risk. In: Department of Public Health EasDoHP, editor. Geneva Switzerland 2016. p. 94.
3. Signorelli L, Patcas R, Peltomaki T, Schatzle M. Radiation dose of cone-beam computed tomography compared to conventional radiographs in orthodontics. *Journal of orofacial orthopedics = Fortschritte der Kieferorthopädie : Organ/official journal Deutsche Gesellschaft für Kieferorthopädie*. 2016;77(1):9-15.
4. Radiation UNSCotEoA. Sources and effects of ionizing radiation: UNSCEAR 2008 Report. New York: United Nations; 2010.
5. Shah N, Bansal N, Logani A. Recent advances in imaging technologies in dentistry. *World journal of radiology*. 2014;6(10):794-807.
6. Forrai J. History of X-ray in dentistry: University of Budapest; 2007.
7. Arai Y, Tammisalo E, Iwai K, Hashimoto K, Shinoda K. Development of a compact computed tomographic apparatus for dental use. *Dentomaxillofac Radiol*. 1999;28(4):245-8.
8. Mozzo P, Procacci C, Tacconi A, Martini PT, Andreis IA. A new volumetric CT machine for dental imaging based on the cone-beam technique: preliminary results. *European radiology*. 1998;8(9):1558-64.
9. Pauwels R. Cone beam CT for dental and maxillofacial imaging: dose matters. *Radiation protection dosimetry*. 2015;165(1-4):156-61.
10. Dawood A, Patel S, Brown J. Cone beam CT in dental practice. *British dental journal*. 2009;207(1):23-8.
11. De Vos W, Casselman J, Swennen GR. Cone-beam computerized tomography (CBCT) imaging of the oral and maxillofacial region: a systematic review of the literature. *Int J Oral Maxillofac Surg*. 2009;38(6):609-25.
12. Brenner DJ, Hall EJ. Computed tomography--an increasing source of radiation exposure. *The New England journal of medicine*. 2007;357(22):2277-84.
13. Li G. Patient radiation dose and protection from cone-beam computed tomography. *Imaging science in dentistry*. 2013;43(2):63-9.
14. W. Bogdanich JCM. Radiation Worries for Children in Dentists' Chairs. *New York Times*. 2010.
15. Loubele M, Bogaerts R, Van Dijck E, Pauwels R, Vanheusden S, Suetens P, et al. Comparison between effective radiation dose of CBCT and MSCT scanners for dentomaxillofacial applications. *European journal of radiology*. 2009;71(3):461-8.
16. Ludlow JB, Davies-Ludlow LE, White SC. Patient risk related to common dental radiographic examinations: the impact of 2007 International Commission on Radiological Protection recommendations regarding dose calculation. *Journal of the American Dental Association (1939)*. 2008;139(9):1237-43.
17. Theodorakou C, Walker A, Horner K, Pauwels R, Bogaerts R, Jacobs R. Estimation of paediatric organ and effective doses from dental cone beam CT using anthropomorphic phantoms. *The British journal of radiology*. 2012;85(1010):153-60.
18. D. K. Maurya TPAD. Role of Radioprotectors in the Inhibition of DNA Damage and Modulation of DNA Repair After Exposure to Gamma-Radiation. In: Chen CC, editor. *Selected Topics in DNA Repair: InTech*; 2011.
19. Lobrich M, Shibata A, Beucher A, Fisher A, Ensminger M, Goodarzi AA, et al. gammaH2AX foci analysis for monitoring DNA double-strand break repair: strengths, limitations and optimization. *Cell cycle (Georgetown, Tex)*. 2010;9(4):662-9.
20. Azzam EI, Jay-Gerin JP, Pain D. Ionizing radiation-induced metabolic oxidative stress and prolonged cell injury. *Cancer letters*. 2012;327(1-2):48-60.
21. Tothova L, Kamodyova N, Cervenka T, Celec P. Salivary markers of oxidative stress in oral diseases. *Frontiers in cellular and infection microbiology*. 2015;5:73.
22. Panier S, Boulton SJ. Double-strand break repair: 53BP1 comes into focus. *Nature reviews Molecular cell biology*. 2014;15(1):7-18.
23. Kinner A, Wu W, Staudt C, Iliakis G. Gamma-H2AX in recognition and signaling of DNA double-strand breaks in the context of chromatin. *Nucleic acids research*. 2008;36(17):5678-94.
24. Ivashkevich A, Redon CE, Nakamura AJ, Martin RF, Martin OA. Use of the gamma-H2AX assay to

- monitor DNA damage and repair in translational cancer research. *Cancer letters*. 2012;327(1-2):123-33.
25. Sedelnikova OA, Rogakou EP, Panyutin IG, Bonner WM. Quantitative detection of (125)IdU-induced DNA double-strand breaks with gamma-H2AX antibody. *Radiation research*. 2002;158(4):486-92.
 26. Horn S, Barnard S, Brady D, Prise KM, Rothkamm K. Combined analysis of gamma-H2AX/53BP1 foci and caspase activation in lymphocyte subsets detects recent and more remote radiation exposures. *Radiation research*. 2013;180(6):603-9.
 27. de Feraudy S, Revet I, Bezrookove V, Feeney L, Cleaver JE. A minority of foci or pan-nuclear apoptotic staining of gammaH2AX in the S phase after UV damage contain DNA double-strand breaks. *Proc Natl Acad Sci U S A*. 2010;107(15):6870-5.
 28. Wang H, Adhikari S, Butler BE, Pandita TK, Mitra S, Hegde ML. A Perspective on Chromosomal Double Strand Break Markers in Mammalian Cells. *Jacobs journal of radiation oncology*. 2014;1(1).
 29. Holmberg O, Czarwinski R, Mettler F. The importance and unique aspects of radiation protection in medicine. *European journal of radiology*. 2010;76(1):6-10.
 30. the UNSCo, Radiation EoA. Sources, effects and risks of ionizing radiation:UNSCEAR 2013 Report. 2013;II Annex B - Effects of radiation exposure of children.
 31. Greenwood TJ, Lopez-Costa RI, Rhoades PD, Ramirez-Giraldo JC, Starr M, Street M, et al. CT Dose Optimization in Pediatric Radiology: A Multiyear Effort to Preserve the Benefits of Imaging While Reducing the Risks. *Radiographics : a review publication of the Radiological Society of North America, Inc*. 2015;35(5):1539-54.
 32. Robertson A, Allen J, Laney R, Curnow A. The cellular and molecular carcinogenic effects of radon exposure: a review. *International journal of molecular sciences*. 2013;14(7):14024-63.
 33. Salmon B, Bardet C, Khaddam M, Naji J, Coyac BR, Baroukh B, et al. MEPE-derived ASARM peptide inhibits odontogenic differentiation of dental pulp stem cells and impairs mineralization in tooth models of X-linked hypophosphatemia. *PLoS One*. 2013;8(2):e56749.
 34. Schindelin J, Arganda-Carreras I, Frise E, Kaynig V, Longair M, Pietzsch T, et al. Fiji: an open-source platform for biological-image analysis. *Nature methods*. 2012;9(7):676-82.
 35. De Vos WH, Van Neste L, Dieriks B, Joss GH, Van Oostveldt P. High content image cytometry in the context of subnuclear organization. *Cytometry Part A : the journal of the International Society for Analytical Cytology*. 2010;77(1):64-75.
 36. Haghdoost S, Czene S, Naslund I, Skog S, Harms-Ringdahl M. Extracellular 8-oxo-dG as a sensitive parameter for oxidative stress in vivo and in vitro. *Free radical research*. 2005;39(2):153-62.
 37. Havelek R, Soukup T, Cmielova J, Seifrtova M, Suchanek J, Vavrova J, et al. Ionizing radiation induces senescence and differentiation of human dental pulp stem cells. *Folia biologica*. 2013;59(5):188-97.
 38. Otmani N. Oral and maxillofacial side effects of radiation therapy on children. *Journal (Canadian Dental Association)*. 2007;73(3):257-61.
 39. Harfouche G, Martin MT. Response of normal stem cells to ionizing radiation: a balance between homeostasis and genomic stability. *Mutation research*. 2010;704(1-3):167-74.
 40. Ferguson DO, Alt FW. DNA double strand break repair and chromosomal translocation: lessons from animal models. *Oncogene*. 2001;20(40):5572-9.
 41. Prise KM, Saran A. Concise review: stem cell effects in radiation risk. *Stem Cells*. 2011;29(9):1315-21.
 42. Muthna D, Soukup T, Vavrova J, Mokry J, Cmielova J, Visek B, et al. Irradiation of adult human dental pulp stem cells provokes activation of p53, cell cycle arrest, and senescence but not apoptosis. *Stem Cells Dev*. 2010;19(12):1855-62.
 43. Arigony AL, de Oliveira IM, Machado M, Bordin DL, Bergter L, Pra D, et al. The influence of micronutrients in cell culture: a reflection on viability and genomic stability. *Biomed Res Int*. 2013;2013:597282.
 44. Metaxas Y, Zeiser R, Schmitt-Graeff A, Waterhouse M, Faber P, Follo M, et al. Human hematopoietic cell transplantation results in generation of donor-derived epithelial cells. *Leukemia*. 2005;19(7):1287-9.
 45. Preethi N, Chikkanarasaiah N, Bethur SS. Genotoxic effects of X-rays in buccal mucosal cells in children subjected to dental radiographs. *Bdj Open*. 2016;2:16001.
 46. Carlin V, Artioli AJ, Matsumoto MA, Filho HN, Borgo E, Oshima CT, et al. Biomonitoring of DNA damage and cytotoxicity in individuals exposed to cone beam computed tomography. *Dentomaxillofac Radiol*. 2010;39(5):295-9.
 47. Angelieri F, de Oliveira GR, Sannomiya EK, Ribeiro DA. DNA damage and cellular death in oral mucosa cells of children who have undergone panoramic dental radiography. *Pediatric radiology*. 2007;37(6):561-5.
 48. Ribeiro DA. Cytogenetic biomonitoring in oral mucosa cells following dental X-ray. *Dentomaxillofac*

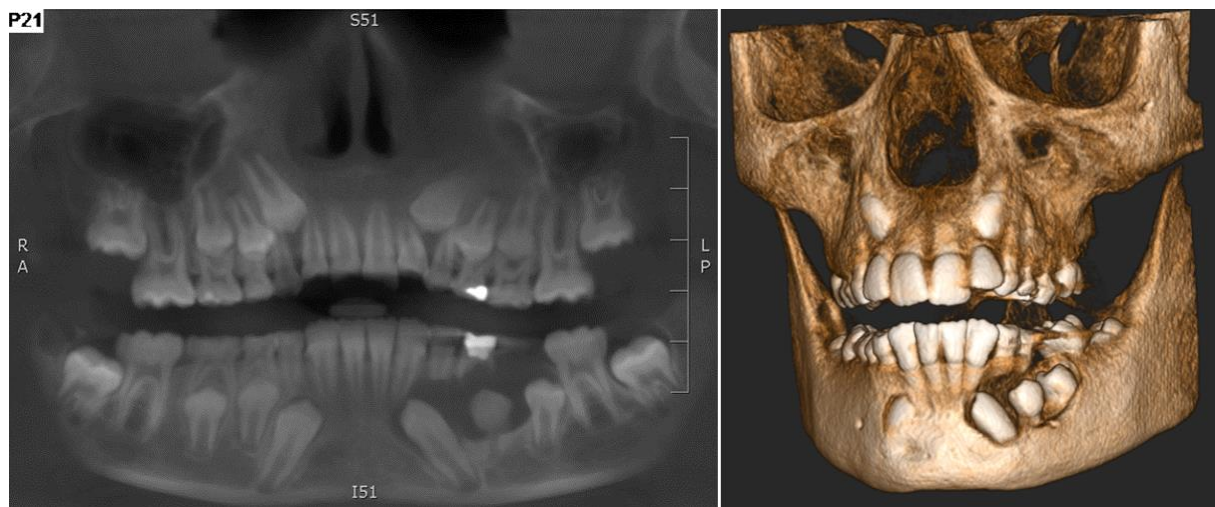
- Radiol. 2012;41(3):181-4.
49. Agarwal P, Vinuth DP, Haranal S, Thippanna CK, Naresh N, Moger G. Genotoxic and cytotoxic effects of X-ray on buccal epithelial cells following panoramic radiography: A pediatric study. *Journal of cytology*. 2015;32(2):102-6.
 50. Yoon AJ, Shen J, Wu HC, Angelopoulos C, Singer SR, Chen R, et al. Expression of activated checkpoint kinase 2 and histone 2AX in exfoliative oral cells after exposure to ionizing radiation. *Radiation research*. 2009;171(6):771-5.
 51. Gonzalez JE, Roch-Lefevre SH, Mandina T, Garcia O, Roy L. Induction of gamma-H2AX foci in human exfoliated buccal cells after in vitro exposure to ionising radiation. *International journal of radiation biology*. 2010;86(9):752-9.
 52. Ramsey MJ, Moore DH, 2nd, Briner JF, Lee DA, Olsen L, Senft JR, et al. The effects of age and lifestyle factors on the accumulation of cytogenetic damage as measured by chromosome painting. *Mutation research*. 1995;338(1-6):95-106.
 53. Ribeiro DA, de Oliveira G, de Castro G, Angeli F. Cytogenetic biomonitoring in patients exposed to dental X-rays: comparison between adults and children. *Dentomaxillofac Radiol*. 2008;37(7):404-7.
 54. Goukassian D, Gad F, Yaar M, Eller MS, Nehal US, Gilchrest BA. Mechanisms and implications of the age-associated decrease in DNA repair capacity. *Faseb j*. 2000;14(10):1325-34.
 55. Sangsuwan T, Haghdoost S. The nucleotide pool, a target for low-dose gamma-ray-induced oxidative stress. *Radiation research*. 2008;170(6):776-83.
 56. Tamura S, Tsukahara H, Ueno M, Maeda M, Kawakami H, Sekine K, et al. Evaluation of a urinary multi-parameter biomarker set for oxidative stress in children, adolescents and young adults. *Free radical research*. 2006;40(11):1198-205.
 57. Kamodyova N, Tothova L, Celec P. Salivary markers of oxidative stress and antioxidant status: influence of external factors. *Disease markers*. 2013;34(5):313-21.
 58. Zhang T, Andrukhov O, Haririan H, Muller-Kern M, Liu S, Liu Z, et al. Total Antioxidant Capacity and Total Oxidant Status in Saliva of Periodontitis Patients in Relation to Bacterial Load. *Frontiers in cellular and infection microbiology*. 2015;5:97.
 59. Umegaki K, Aoki S, Esashi T. Whole body X-ray irradiation to mice decreases ascorbic acid concentration in bone marrow: comparison between ascorbic acid and vitamin E. *Free radical biology & medicine*. 1995;19(4):493-7.
 60. M. Battino MSF, I. Gallardo, H. N. Newman, P. Bullon. The antioxidant capacity of saliva. *Journal Of Clinical Periodontology*. 2002:189-94.
 61. Moore S, Calder KA, Miller NJ, Rice-Evans CA. Antioxidant activity of saliva and periodontal disease. *Free radical research*. 1994;21(6):417-25.
 62. Sies H. Total antioxidant capacity: appraisal of a concept. *The Journal of nutrition*. 2007;137(6):1493-5.

7 Supplemental information



Supplementary figure 1: Annual average exposure to ionizing radiation and the associated contribution of different radiation sources.

In Belgium 45.8% of the average annual exposure to IR is caused by medical application, 34.0% by radio-active gases (radon or thoron), 8.0% by radioactive material present in soil, rocks and buildings, 6.0% from our food (potassium 40), 5.9% cosmic radiation and 0.4% from nuclear industry Worldwide 19.8% of the average annual exposure to IR is caused by medical application, 41.7% by radon, 15.9% by radioactive material present in soil, rocks and buildings, 9.6% from our food, 12.9% cosmic radiation and 0.2% from nuclear industry or fall out from nuclear weapon testing *Source: Adapted from FANC (1) / UNSCEAR (4).*



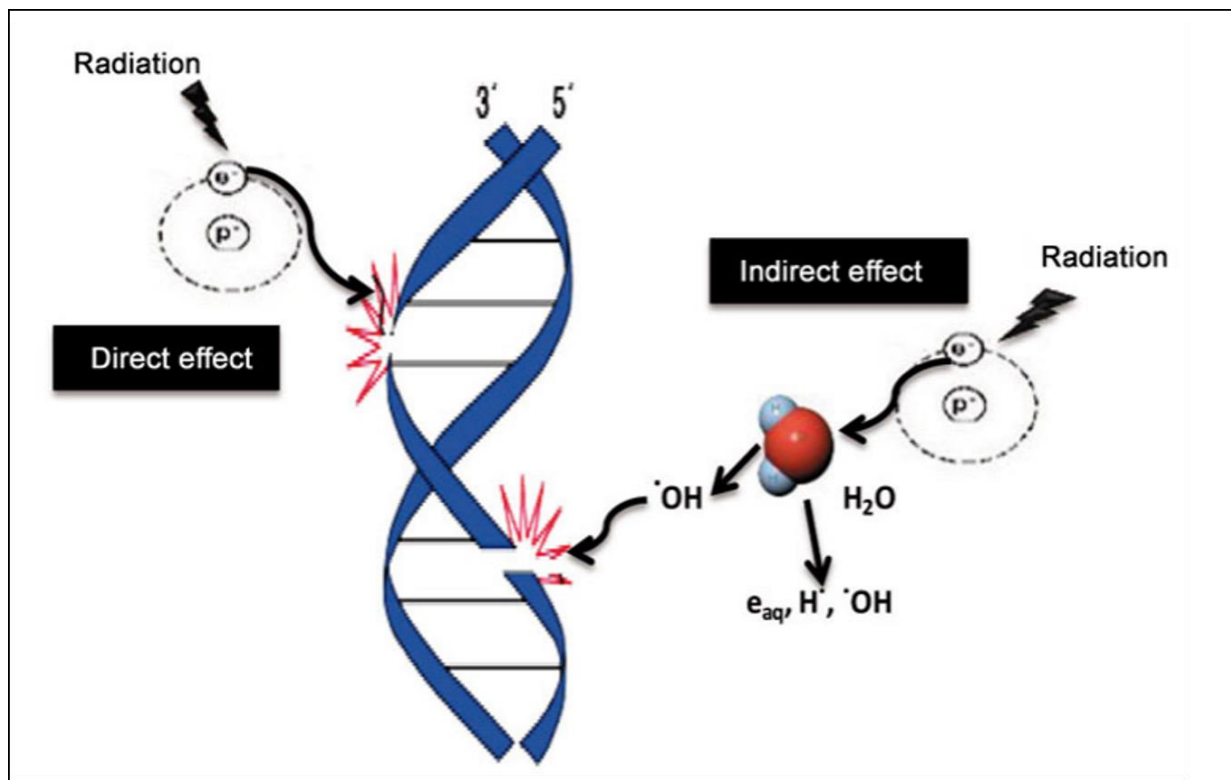
Supplementary figure 2: 2D and 3D images of the oral and maxillofacial region.

On the left: 2D image of the maxillofacial region from panoramic radiograph. On the right: 3D reconstruction of the maxillofacial region based on dental CBCT data. *Courtesy of Prof. R. Jacobs (Oral and Maxillofacial Surgery – Imaging and Pathology, Katholieke Universiteit Leuven).*

Supplementary table 1: Typical effective dose associated with diagnostic imaging examinations (2).

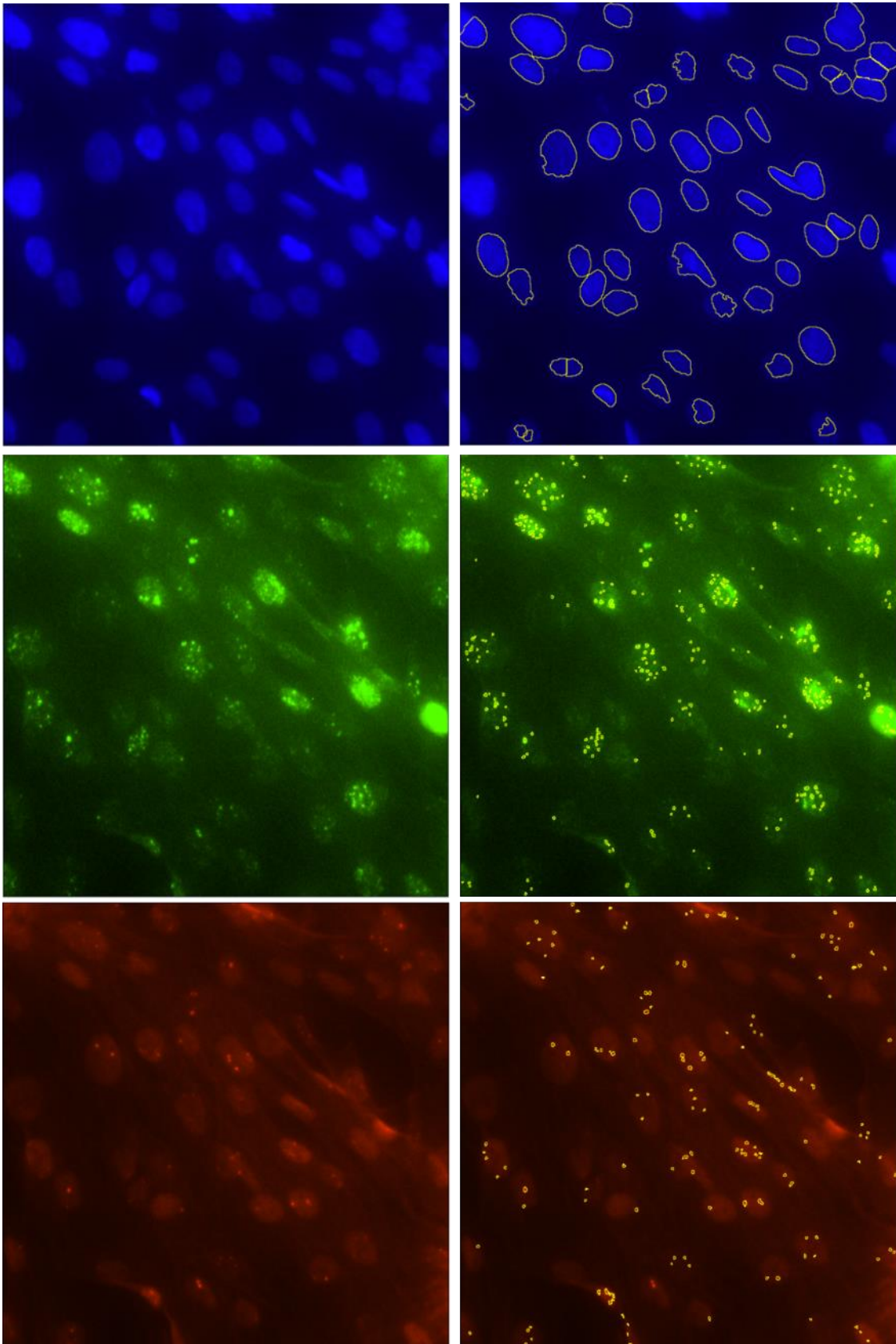
Source: adapted from WHO 2016.

Diagnostic procedure	Typical effective dose
<i>head CT</i>	
Adult	2 mSv
1 year old	3.7 mSv
10 year old	2.2 mSv
<i>Dental examinations</i>	
Intra-oral radiography	0.005 mSv
Panoramic radiography	0.01 mSv
Craniofacial CBCT	<1 mSv



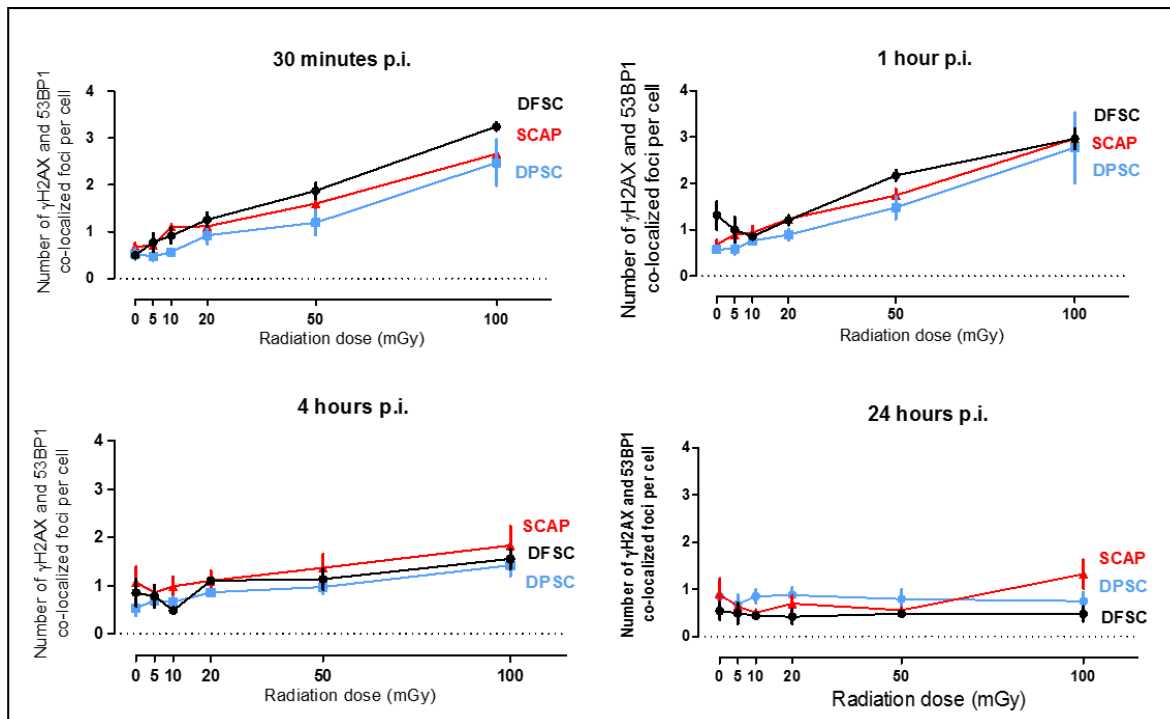
Supplementary figure 3: Direct and indirect effects of ionizing radiation on DNA.

Ionizing radiation can directly damage the DNA or indirectly through radiolysis of water, thereby generating reactive oxygen species.



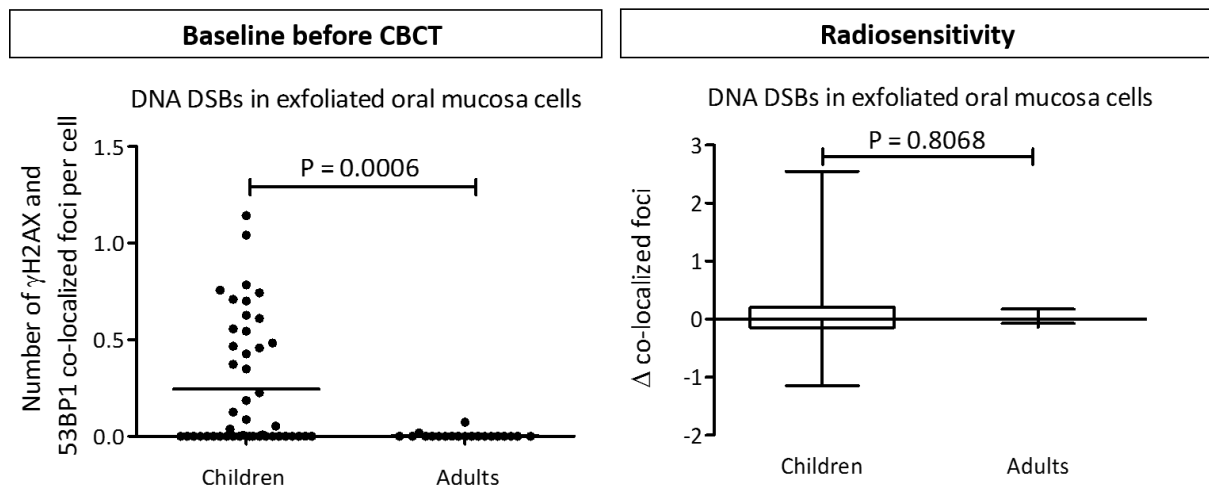
Supplementary figure 4: Automated foci count using FIJI software.

Blue = DAPI, green = γ H2AX, red = 53BP1. The nuclei of the cells were identified based on the DAPI stain. On the right the region of interest (nucleus) is marked. Identification and analysis of the 53BP1 and γ H2AX foci was performed in an automated manner. Only foci within the region of interest (nucleus) were counted.



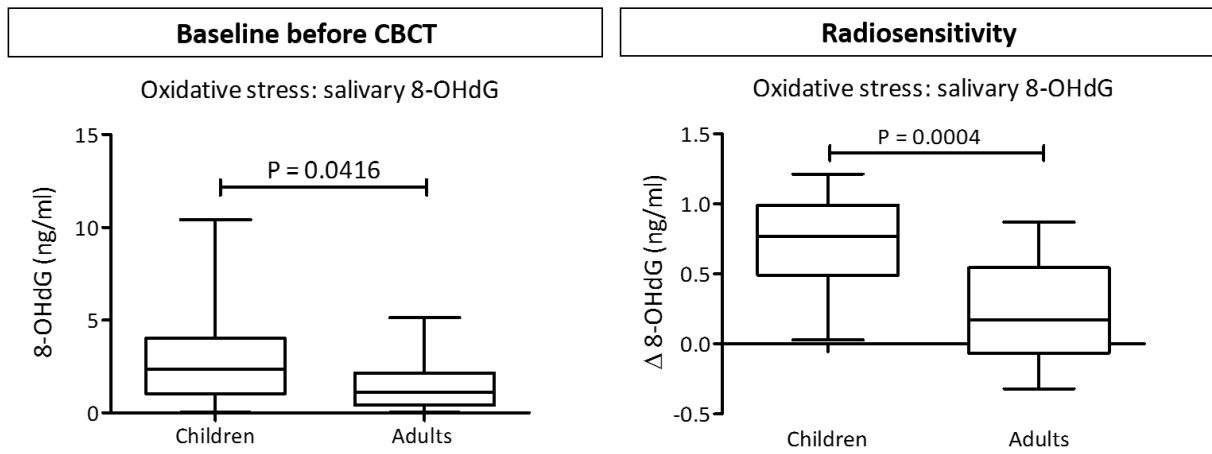
Supplementary figure 5: Dose response relationship of DPSC, DFSC and SCAPs 30 min, 1 h, 4 hrs and 24 hrs p.i..

DNA DSBs were quantified with a γ H2AX and 53BP1 double immunofluorescence staining. Linear regression of DNA DSB induction shows the mean number of co-localized foci per cell nucleus in DPSC (blue), SCAP (red) and DFSC (black) 30 min, 1 h, 4 hrs and 24 hrs after X-ray exposure. (DPSC: $R^2 = 0.9730$, $R^2 = 0.9916$, $R^2 = 0.9639$; DFSC: $R^2 = 0.9938$, $R^2 = 0.9141$, $R^2 = 0.7540$; SCAP: $R^2 = 0.9798$, $R^2 = 0.9950$, $R^2 = 0.9444$). The slope decreased over time returning to a constant basal response 24 hrs p.i. ($R^2 = 0.07794$, $R^2 = 0.01300$, $R^2 = 0.4737$). Data are expressed as mean \pm S.E.M. DPSC = dental pulp stem cells, DFSC = dental follicle stem cells, SCAP = stem cells of the apical papilla. S.E.M = Standard error of the mean.



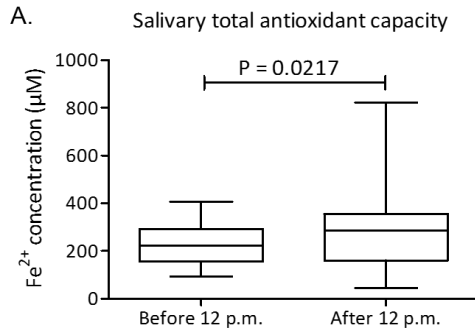
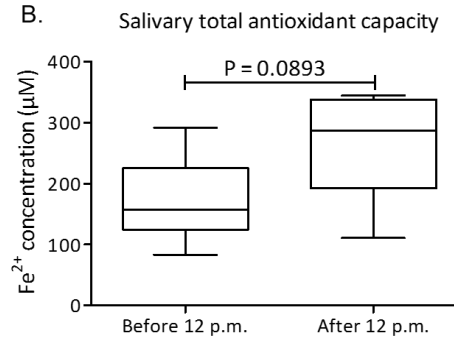
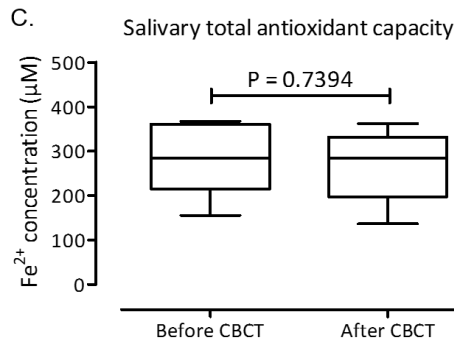
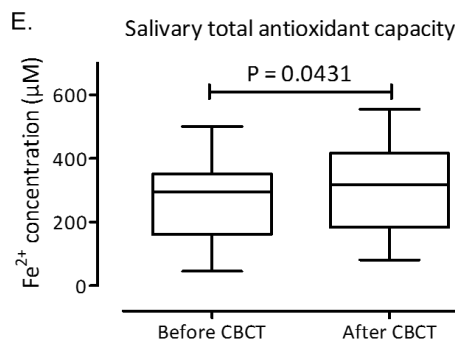
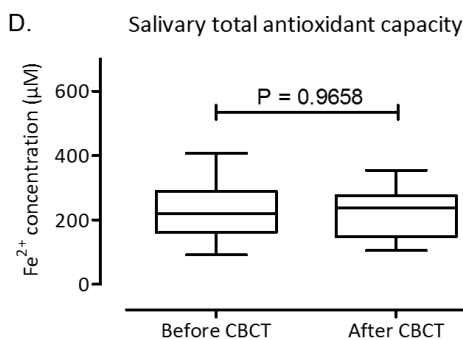
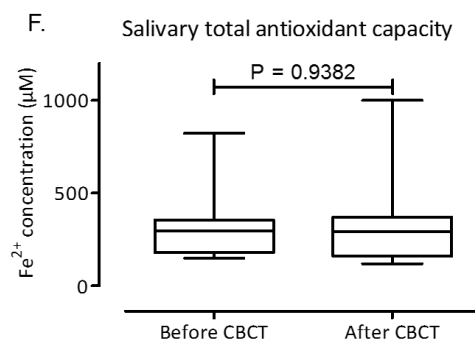
Supplementary figure 6: Comparison of basal DNA DSB occurrence and radiation sensitivity between children and adults.

Exfoliated oral mucosa cells were collected immediately before dental CBCT exposure from paediatric ($n = 47$) and adult ($n = 20$) patients. The mean number of γ H2AX and 53BP1 co-localized foci was determined with a double immunofluorescence staining. The occurrence of co-localized foci, measured before dental CBCT exposure, was higher in children than in adults ($p = 0.0006$). The radiation sensitivity was determined by comparing the response (Δ : after CBCT - before CBCT) between children and adults. The response observed in children and adults was the same ($p = 0.9053$). Data was analysed with a Mann Whitney test. CBCT = cone beam computed tomography, DSB = double strand break.



Supplementary figure 7: Comparison of basal salivary 8-OHdG and radiation sensitivity between children and adults.

Saliva samples were collected from children and adults before and 30 minutes after dental CBCT exposure. 8-OHdG concentration was measured with a competitive ELISA-assay. Comparison of the basal level of 8-OHdG between children and adults shows that the basal level of 8-OHdG, measured before dental CBCT, is significantly higher in children ($p = 0.0416$). Furthermore, the radiation sensitivity of children and adults was compared by comparing the response (Δ : after CBCT - before CBCT) between the two groups. There was no difference in radiation sensitivity between children and adults ($p = 0.0004$). Data was analysed with an unpaired t test with Welch's correction (baseline) and an unpaired t-test of log transformed data (radiation sensitivity). ELISA = Enzyme Linked Immunosorbent Assay, CBCT = cone beam computed tomography, 8-OHdG = 8-hydroxy-2'-deoxyguanosine.

Children: baseline before vs. after 12 p.m.**Adults: baseline before vs. after 12 p.m.****Girls before 12 p.m.****Girls after 12 p.m.****Boys before 12 p.m.****Boys after 12 p.m.****Supplementary figure 8: Meta-analysis of total antioxidant capacity data in saliva before and after dental CBCT exposure.**

Saliva samples were collected from children and adults before and 30 minutes after dental CBCT exposure. The FRAP-assay was used to determine the TAC. TAC is expressed as Fe²⁺ concentration based on internal iron standard. **A-B:** The basal TAC was compared between saliva samples collected before 12 p.m. and saliva samples collected after 12 p.m. in both children and adults. In the paediatric population, the basal level of TAC measured after 12 p.m. was significantly higher than the TAC measured before 12 p.m. ($p = 0.0217$). The same trend was observed in adults ($p = 0.0893$). Data was analysed with an unpaired t-test with Welch's correction (children) and a Mann Whitney test (adults). **C-D:** All children were divided into two groups based on the time of their CBCT examination. No significant difference was observed between the TAC before and after dental CBCT ($p = 0.7394$, $p = 0.9658$) in both girls and boys who had their examination before 12 p.m. Data was analysed with a paired t-test (girls) and a non-parametric Wilcoxon signed-rank test (boys). **E-F:** No significant difference was observed between the TAC before and after dental CBCT in boys who had their examination after 12 p.m. ($P = 0.9382$). In the group of girls who had their examination after 12 p.m. a significant increase in TAC after dental CBCT was observed. Data was analysed with a paired t-test (girls) and a non-parametric Wilcoxon signed-rank test (boys). TAC = total antioxidant capacity, CBCT = cone beam computed tomography.

Auteursrechtelijke overeenkomst

Ik/wij verlenen het wereldwijde auteursrecht voor de ingediende eindverhandeling:
Dental paediatric imaging: an investigation into low dose radiation-induced risks

Richting: **master in de biomedische wetenschappen-klinische moleculaire wetenschappen**
Jaar: **2017**

in alle mogelijke mediaformaten, - bestaande en in de toekomst te ontwikkelen - , aan de Universiteit Hasselt.

Niet tegenstaand deze toekenning van het auteursrecht aan de Universiteit Hasselt behoud ik als auteur het recht om de eindverhandeling, - in zijn geheel of gedeeltelijk -, vrij te reproduceren, (her)publiceren of distribueren zonder de toelating te moeten verkrijgen van de Universiteit Hasselt.

Ik bevestig dat de eindverhandeling mijn origineel werk is, en dat ik het recht heb om de rechten te verlenen die in deze overeenkomst worden beschreven. Ik verklaar tevens dat de eindverhandeling, naar mijn weten, het auteursrecht van anderen niet overtreedt.

Ik verklaar tevens dat ik voor het materiaal in de eindverhandeling dat beschermd wordt door het auteursrecht, de nodige toelatingen heb verkregen zodat ik deze ook aan de Universiteit Hasselt kan overdragen en dat dit duidelijk in de tekst en inhoud van de eindverhandeling werd genotificeerd.

Universiteit Hasselt zal mij als auteur(s) van de eindverhandeling identificeren en zal geen wijzigingen aanbrengen aan de eindverhandeling, uitgezonderd deze toegelaten door deze overeenkomst.

Voor akkoord,

Gilles, Liese

Datum: **8/06/2017**